

# Decay properties of $1p$ -shell hypernuclei. I. Excited bound states

J. Žofka

*Institute of Nuclear Physics, Czechoslovak Academy of Sciences, Řež, Czechoslovakia*

L. Majling

*Joint Institute for Nuclear Research, Dubna; Institute of Nuclear Physics, Czechoslovak Academy of Science, Řež, Czechoslovakia*

V. N. Fetisov

*P. N. Lebedev Physics Institute, USSR Academy of Sciences, Moscow*

R. A. Éramzhan

*Institute of Nuclear Research, USSR Academy of Sciences, Moscow*

Fiz. Elem. Chastits At. Yadra **22**, 1292–1346 (November–December 1991)

The general concept of a shell model is applied to the description of light hypernuclei, and a shell approach in hypernuclear spectroscopy is formulated in a translationally invariant form. It is noted that the developed formalism of a translationally invariant shell model is universal for the description of the excitation of hypernuclear levels and also their decay properties. Other approaches in the theory of hypernuclear structure are briefly discussed. The review includes new theoretical results on the  $\gamma$  spectroscopy of hypernuclei of interest for further experiments.

## INTRODUCTION

The physics of hypernuclei, as a separate field at the borderline of nuclear physics and elementary-particle physics, arose almost 40 years ago. The initial long period of accumulation of data, mainly on the binding energies of the  $\Lambda$  hyperon and the weak decay modes of the ground states of light hypernuclei,<sup>1</sup> was followed in the seventies by a stage of rapid establishment and development of hypernuclear spectroscopy.<sup>2–5</sup> This was made possible by the development of sufficiently intense beams of  $K$  mesons, the application of modern counter methods, and the use, in  $(K^-, \pi^-)$  reactions, of specially developed magnetic spectrometers to detect mesons with high momenta. Because of the small momentum transfers characteristic of them,  $(K^-, \pi^-)$  reactions proved to be especially effective in investigations of excited levels of hypernuclei.<sup>6</sup> The most important directions of hypernuclear research and interactions of strange particles are regularly reflected in the proceedings of international conferences and symposia.<sup>7–13</sup>

Systematic investigations, begun at CERN<sup>14</sup> and continued at the Brookhaven National Laboratory (BNL, USA),<sup>15</sup> made it possible to obtain extensive information on the excitation spectra of many  $\Lambda$  hypernuclei from  ${}^6_\Lambda\text{Li}$  to  ${}^{209}_\Lambda\text{Bi}$  up to energies 20–30 MeV. At the beginning of the eighties, investigations at these laboratories of  $(K^-, \pi^-)$  reactions on the light target nuclei  ${}^6\text{Li}$ ,  ${}^9\text{Be}$ ,  ${}^{12}\text{C}$ , and  ${}^{16}\text{O}$  revealed the existence of very narrow resonances with width  $\Gamma \lesssim 10$  MeV (Ref. 16) which, in accordance with the initial ideas,<sup>17</sup> were taken to represent the discovery of excited  $\Sigma$  hypernuclei. At the present time, the interpretation of these peaks is contradictory. Because of the limited amount of experimental data and their low accuracy, it is still not clear whether the observed peaks are true hypernuclear resonances or whether they are due to threshold effects in quasifree production of  $\Lambda$  hyperons (Ref. 18).<sup>1</sup>

In recent years, there has been a further extension of investigations of hypernuclear physics, due in the first

place to success in exploiting new reactions to produce hypernuclei. First experiments on the spectroscopy of  $\Lambda$  hypernuclei using pion beams in  $(\pi^+, K^+)$  reactions with momentum  $P_\pi \gtrsim 1$  GeV/ $c$  have been realized at BNL.<sup>21</sup> In Japan, a method for studying hypernuclear spectra in  $(K^-, \pi^\mp)$  reactions associated with capture of stopped kaons from mesoatomic orbits is being perfected.<sup>22</sup> At the Joint Institute for Nuclear Research (Dubna, USSR), the first successful experiments on the production of relativistic  ${}^4_\Lambda\text{H}$  hypernuclei and measurement of their lifetime in collisions of relativistic ions have been made.<sup>23</sup> Data on the lifetimes of heavy hyperfragments ( $A \approx 200$ ) have been obtained at CERN at the LEAR facility in reactions involving absorption of antiprotons by nuclei<sup>24</sup> and at Khar'kov<sup>25</sup> in electron bombardment of nuclei. Experiments involving photoproduction of hypernuclei, which are very promising for spectroscopic investigations, are being discussed at the P. N. Lebedev Physics Institute<sup>26</sup> and at Laboratories in Japan and Italy.<sup>27</sup> At KEK (Japan) it is planned to study the properties of polarized hypernuclei in  $(\pi^+, K^+)$  reactions.<sup>28</sup> Hypernuclear investigations will be among the most important in the research programs for the planned new class of accelerators (KAON-TRIUMF, Canada; LAMPF-II, USA), hadron factories,<sup>29</sup> and the high-current electron accelerator under construction in the USA (CEBAF Laboratory).<sup>30</sup> Thus, numerous major nuclear laboratories already perform or plan to begin extensive investigations in the field of hypernuclear physics.

As new methods of producing hypernuclei are mastered, new pages are opened in the spectroscopy of  $\Lambda$  hypernuclei. For example, in  $(\pi^+, K^+)$  reactions it proved possible to observe the theoretically predicted<sup>3,31</sup> bands of hypernuclear levels corresponding to the single-particle spectrum of  $\Lambda$ -hyperon states in the nuclear field.<sup>21</sup> These experimental results represent valuable data for testing shell ideas about the properties of nuclear systems at the level of both nucleonic and quark degrees of freedom.<sup>32</sup> Hypernuclear experiments using beams of relativistic

ions<sup>23,33</sup> are an important tool for studying individual modes of the weak decays of light hypernuclei. They gave a stimulus to new theoretical elaboration of the mechanism of hypernuclear production (coalescence model).<sup>34</sup> The results of experiments using antiproton and electron beams are important for understanding the weak-decay dynamics of heavy hyperfragments.<sup>35,36</sup>

There has been further development and study of the decay properties of hypernuclear levels due to the strong, electromagnetic, and weak interactions.

Recent studies at BNL of  $(K^-, \pi^-)$  reactions "in flight" led to the detection of  $\gamma$  rays from the deexcitation of bound states of the hypernuclei  ${}^7_\Lambda\text{Li}$  and  ${}^9_\Lambda\text{Be}$  (Ref. 37). The interpretation of these  $\gamma$  lines made it possible to obtain more realistic potential parameters of the shell model for light hypernuclei.<sup>38</sup> In the case of the lithium target, the investigation also detected secondary  $\gamma$  rays accompanying the decay of the hypernuclear resonance; these are of interest for determining the configuration content of the hypernuclear wave function. In the experiments of Ref. 37, in contrast to the pioneering CERN studies,<sup>39-41</sup> in which the energies of the  $\gamma$  rays from  ${}^4_\Lambda\text{H}$  ( ${}^4_\Lambda\text{He}$ ) deexcitation were measured, it was possible to progress further and identify the energy region of excitation of the original hypernucleus. This new aspect of the experiment is particularly valuable for determining the structure of the resonance, which determines the probabilities of decays through baryonic channels with population of excited levels of daughter nuclei or hypernuclei. In this way, it was possible to establish for the  ${}^7\text{Li}$  target nucleus a chain of excitation and baryonic decay processes, and this made it possible to relate unambiguously the hypernuclei  $\gamma$  rays to the emitter fragment ( ${}^4_\Lambda\text{He}$ ) and identify nuclear  $\gamma$  rays from deexcitation of the state  ${}^6\text{Li}(0^+, 1; 3.56 \text{ MeV})$  formed on emission of the  $\Lambda$  hyperon. This experiment confirmed the mechanism suggested in Ref. 42 for formation of  ${}^4_\Lambda\text{H}$  and  ${}^4_\Lambda\text{He}$  hypernuclei for a lithium target based on cluster decay of a resonance with configuration  $\{s^3p^2 \otimes s_\Lambda\}$ . The nuclear  $\gamma$  rays from  ${}^6\text{Li}$  deexcitation detected in the same experiment found a natural explanation as a manifestation of isospin selection rules in the  $\gamma$  decay of the hypernuclear resonance  ${}^7_\Lambda\text{Li}(3^-, 2, T=1; 13.0 \text{ MeV})$ .<sup>43</sup> This is an interesting point in study of hypernuclear properties, since the problem of the "purity" of isospin in hypernuclei has been little studied, and isospin symmetry can be broken both by the Coulomb interaction of the protons in the core nucleus and by the presence in the  $\Lambda N$  forces of a component that breaks the charge symmetry.<sup>44</sup>

At BNL, the first results have been obtained<sup>45,46</sup> from a measurement of the lifetimes of daughter product hypernuclei produced as a result of baryonic decays of hypernuclei excited in  $(K^-, \pi^-)$  reactions. These experiments also determined the energy region of excitation of the hypernuclear resonance. Such a method makes it possible to identify the  $\Lambda$  decay channel and the channel of mesonless decay of the daughter hypernucleus through the  $\Lambda N \rightarrow NN$  weak process. The measurements provided confirmation of the theory of baryonic decays of  ${}^6\text{Li}$  (Ref. 42), in which an important part is played by the supermultiplet structure of

the hypernuclear states in conjunction with selection rules in accordance with a Young diagram, this being reflected in suppression of  $\Lambda$  emission on decay of a resonance with energy  $\approx 18 \text{ MeV}$  (see also Rev. 47). The permutational symmetry properties of the hypernuclear wave function also control the cluster decay of states with configuration  $\{s^3p^8 \otimes s_\Lambda\}$  in  ${}^{12}_\Lambda\text{C}$  with  ${}^3\text{He}$  emission.<sup>48</sup> These considerations were decisive in the identification of the daughter hypernucleus  ${}^9_\Lambda\text{Be}$ , whose weak decay was observed in the experiment of Ref. 45.

Finally, in very recent experiments at KEK<sup>49</sup> in reactions involving the absorption of stopped  $K^-$  mesons by the  ${}^7\text{Li}$ ,  ${}^9\text{Be}$ ,  ${}^{12}\text{C}$ , and  ${}^{16}\text{O}$  nuclei an appreciable  ${}^4_\Lambda\text{H}$  yield was observed even though the threshold energies for such decay are much higher than the nucleon and hyperon threshold energies. This channel was reliably identified through the detection of pions with momentum  $\approx 132.9 \text{ MeV}/c$  from the decay  ${}^4_\Lambda\text{H} \rightarrow \pi^- + {}^4\text{He}$ . As yet, there is no ambiguous explanation of these data. Theoretical investigation of the structure of highly excited hypernuclear resonances<sup>42,50</sup> suggests that the interpretation of the observed  ${}^4_\Lambda\text{H}$  yield must take into account fragmentation of the hypernuclear daughter  $s$  levels together with a possible contribution of pion charge-exchange processes in the final state.<sup>51</sup> The compound-hypernucleus model proposed in Ref. 49 is also not ruled out.

These examples of realized experiments show clearly the need that already exists for a comprehensive study of all the problems associated with the mechanism of production of hypernuclei, the structure of the produced hypernuclear states, and the details of their decay. Admittedly, the presently existing technical limitations due to the low intensity of the kaon beams and the use of thick targets have the consequence that one can detect efficiently only neutral particles ( $\gamma$  rays, the  $\Lambda$  hyperon, neutrons) and pions or fast nucleons resulting from hyperfragment weak decay.

It is obvious that reliable interpretation of reactions requires from theory knowledge of all decay channels, including the as yet undetected channels with emission of slow charged particles. As a theory sufficiently universal for application to hypernuclei, the present authors have developed the translationally invariant shell model (TISM).

In this review, which consists of two parts, we concentrate our main attention on the decay properties of the hypernuclei. This problem of hypernuclear spectroscopy is very important, since the understanding of the principal features of baryonic decays and electromagnetic transitions is intimately related to the elucidation of the configuration structure of the hypernuclear states and details of the hyperon-nucleon interactions.

The first part of the review covers the basic ideas and formalism of the ordinary and the translationally invariant hypernuclear shell model; there is a brief discussion of other approaches in the theory of hypernuclear structure and detailed consideration of the most recent investigations of  $\gamma$  spectroscopy and some questions related to this theme.

In part II of the review, together with a discussion of



various processes of hypernuclear production, the main attention will be devoted to baryonic decays of excited hypernuclear levels corresponding to the  $1\hbar\omega$  configuration  $\{s^4 p^n \otimes p_\Lambda\}$ , the  $\gamma$  spectroscopy of the daughter hypernuclei and nuclei, the comparison of the results of the shell model with bound states with the results of a model that takes into account the continuous spectrum, and also some effects due to the influence of the shell structure on weak mesonless decays of the ground and isomer states of hypernuclei.

## 1. BASIC IDEAS OF THE SHELL MODEL OF LIGHT HYPERNUCLEI

The preceding stage in the development of hypernuclear physics showed that the use of a many-particle shell model that takes into account the configurations of all  $A$  nucleons makes it possible to describe many important aspects of hypernuclear structure, the spectrum and excitation intensity of the levels in different reactions, and also the nature of the subsequent decay of the produced states. Therefore, our analysis is based on a many-particle shell model developed in detail for hypernuclei of the  $1p$  shell ( $6 \leq A \leq 16$ ). It is well known that many states of ordinary nuclei and hypernuclei possess clearly expressed cluster properties.<sup>53-55</sup> The many-particle shell model reflects quite well the main qualitative aspects of the association of nucleons in the framework of the classification of nuclear states by means of Young diagrams.<sup>56,57</sup> Of course, to describe hypernuclear properties such as the compression or deformation of cluster systems in the presence of the  $\Lambda$  hyperon it is necessary to use a cluster model or the resonating-group method.<sup>53</sup>

To describe the excited hypernuclear states of the type  $|(l_j n)^{-1}(l_j \Lambda): \mathcal{J}\rangle$  (hyperon particle, nucleon hole), which are formed in  $(K^-, \pi^-)$  or  $(\pi^+, K^+)$  reactions, it is expedient to use the *translationally invariant shell model* (TISM).<sup>56</sup> The use of Jacobi variables in the TISM radial wave functions makes it possible to determine the type of "carrier" of the excitation: the center of mass of the system, the hyperon, a nucleon, or collective motion. Different types of excitations are related by simple kinematic transformations from one set of Jacobi variables to another. In such a formalism, one can investigate the nucleonic decay channel corresponding to excitation of the hyperon (see Sec. 2). Of course, in the framework of the TISM there is automatic elimination of "spurious" states associated with motion of the center of mass of the complete system in excited  $n\hbar\omega$  states ( $n > 0$ ).

Most of the hypernuclear resonances produced in  $(K^-, \pi^-)$  reactions are in the continuous spectrum. However, as is shown by analysis of the excitation functions and decay characteristics of the resonances,<sup>58-60</sup> a decisive role in their interpretation is played by structure effects, which in many cases are so strong that the specific continuum problems recede into the background. Therefore, we shall use a shell model with bound single-particle states. As one of the most striking examples illustrating the effectiveness of the use of this form of the model, we can again mention the  ${}^6_\Lambda\text{Li}$  hypernucleus.<sup>42</sup> In the framework of the TISM

with bound states, it was possible to explain the gross structure of the observed excitation spectrum; moreover, nontrivial predictions were made concerning the main decay channels of the resonances, which, as we noted in the Introduction, were confirmed in subsequent measurements.<sup>46,61,62</sup>

Before we discuss the TISM formalism for hypernuclei and the structure of the excited levels and their decays, it is convenient to divide the set of states of  $1p$ -shell hypernuclei into three groups:

*States of normal parity* ( $p^{-1}s_\Lambda$ ), in which the hyperon is in the lowest  $0s$  orbit, and in the nuclear core the  $0s$  orbit is completely occupied. This is the so-called  $0\hbar\omega$  excitation band of the hypernucleus. It corresponds to the configuration  $\{s^4 p^{k-1}; e \otimes s_\Lambda: \mathcal{J} T\}$  or, succinctly,  $(p^{-1}s_\Lambda)$ . Here, the symbol  $e$  denotes the energy  $E$ , the total angular momentum  $J$ , and the isospin  $T$  of the nuclear subsystem. The last notation emphasizes that the  $1p$  nucleon is replaced by the  $\Lambda$  hyperon. The ground and, as a rule, excited bound states correspond to such a configuration. The main deexcitation channels of these states are electromagnetic and weak (for the ground and isomer states) decays. States of this nature are used to determine the parameters of the residual  $\Lambda N$  interaction in the hypernuclear shell model.

*States of anomalous parity* ( $p^{-1}p_\Lambda$ ), in which the hyperon is in the  $1p$  orbit and in the nuclear core the  $0s$  orbit is again completely occupied. This is the so-called  $1\hbar\omega$  excitation band of the hypernucleus. It corresponds to the configuration  $\{s^4 p^{k-1}; e \otimes p j_\Lambda: \mathcal{J} T\}$  or, in the abbreviated form,  $(p^{-1}p_\Lambda)$ . States with such a configuration are strongly excited in  $(K^-, \pi^-)$  substitution reactions.

Study of the spectrum of  $(p^{-1}p_\Lambda)$  states makes it possible to augment the information about the parameters of the residual  $\Lambda N$  interaction—the range of the  $\Lambda N$  forces, their Majorana component, etc. For the example of the  $(p^{-1}p_\Lambda)$  states, it is possible to investigate the conditions of formation and excitation of "analog" states, which possess the same orbital symmetry as states of  $k$  nucleons in the  $1p$  shell, and *genuinely hypernuclear states*, which possess a high orbital symmetry (Young diagram with five columns) and which are sometimes called supersymmetric.<sup>53,63</sup>

*States of anomalous parity* ( $s^{-1}s_\Lambda$ ) belonging to the  $1\hbar\omega$  band when the hyperon is in the lowest  $0s$  orbit and there is one hole in the  $0s$  state of the nuclear core. Such states correspond to the configuration  $\{s^3 p^k; e \otimes s_\Lambda: \mathcal{J} T\}$  or, in the abbreviated notation,  $(s^{-1}s_\Lambda)$ .

The  $1\hbar\omega$  band also includes states with the more complicated structure  $\{s^4 p^{k-2}(2s, 2d); e \otimes s_\Lambda: \mathcal{J} T\}$  [in the other notation,  $(p^{-2}ls_\Lambda)$ ,  $l=2s$  or  $2d$ ], which, by virtue of the single-particle reaction mechanism, are not excited in the  $(K^-, \pi^-)$  process but can influence the fragmentation of the resonances and the probabilities of nucleonic decays. In the standard shell model, it is necessary to include such configurations in order to construct states that are "pure" with respect to the center-of-mass motion. It is obvious that in the TISM the kinematic correlations are automatically taken into account in the construction of the basis functions. An additional contribution to the resonance

wave function of states with configuration  $(p^{-2}s_\Lambda)$  arises in the TISM only when these states are strongly mixed by the  $\Lambda N$  interaction (dynamic correlations) with the states with configurations  $(p^{-1}p_\Lambda)$  or  $(s^{-1}s_\Lambda)$  mentioned above. In the literature, the  $(p^{-2}s_\Lambda)$ -configuration states have become known as intruder states.

If the single-particle potentials for the  $\Lambda$  hyperon and nucleon were the same, then all the  $1\hbar\omega$  configurations  $(p^{-1}p_\Lambda)$ ,  $(s^{-1}s_\Lambda)$ , and  $(p^{-2}s_\Lambda)$  would be degenerate with respect to the energy. In reality, this is not the case—the experimental data on the excitation functions of hypernuclei<sup>2,61</sup> and theoretical calculations<sup>64,65</sup> show that the well depth for the hyperon is significantly less than for the nucleon, and the corresponding hyperon single-particle energies are approximately half the nucleon energies. Therefore, the states with configuration  $(s^{-1}s_\Lambda)$  must lie above the  $(p^{-1}p_\Lambda)$  states. Without going into detailed estimates of the configuration splitting in hypernuclei, which, as is well known, also occurs in ordinary nuclei,<sup>66</sup> we merely mention that in the limit of weak binding of the hyperon to the nuclear core,<sup>58</sup> which describes approximately the spectra of the hypernuclei in  $(K^-, \pi^-)$  reactions at small pion emission angles, excitation energies of about 10–15 MeV correspond to the  $(p^{-1}p_\Lambda)$  states, and energies 18–30 MeV to the  $(s^{-1}s_\Lambda)$  states. Actual calculations<sup>42,67,68</sup> show that the residual  $\Lambda N$  interaction does not mix these groups of levels too strongly. Because there are only two neutrons in the 0s shell of the target nuclei, the  $(s^{-1}s_\Lambda)$  configurations are clearly manifested only in the light hypernuclei  ${}^6_7\text{Li}$ ,  ${}^9_\Lambda\text{Be}$ ,  ${}^{12,13}_\Lambda\text{C}$  (Ref. 69).

It is well known<sup>42,47</sup> that states with  $(s^{-1}s_\Lambda)$  configuration are subject to specific structural hindrances to baryonic decays (they will be discussed in more detail in the second part of the review): Hyperon emission is forbidden (such decay is possible only through admixture of the  $(p^{-1}p_\Lambda)$  configuration); emission of an  $\alpha$  particle or  ${}^5_\Lambda\text{He}$  hyperfragment is forbidden (Young-diagram selection rules); there is strong suppression of the nucleonic channel (decay is possible by virtue of kinematic correlations); there is enhancement of the decay channels with emission of  ${}^3\text{He}$  ( ${}^3\text{H}$ ) nuclei and  ${}^4_\Lambda\text{He}$  ( ${}^4_\Lambda\text{H}$ ) hyperfragments.

In discussion of the decay characteristics of highly excited hypernuclear resonances, one must therefore bear in mind the  $(s^{-1}s_\Lambda)$  configuration.

In recent experiments, hypernuclei have been produced by means of the new reactions  $(\pi^+, K^+)$ ,  $(K^-_{\text{stop}}, \pi^-)$ , in which highly excited states are predominantly populated. For the particle-hole identification of these states, it is entirely sufficient to use the classification of states in the *standard shell model* (SSM). However, for analysis of the decay characteristics of the levels the advantages of the translationally invariant shell model are obvious.

The translationally invariant shell model developed by the authors for hypernuclei is a completely universal model in the sense that it describes the spectroscopic properties of all the listed groups of states on a unified basis. We note that the standard (translationally noninvariant) shell model has been applied by many authors to the description

of hypernuclear level spectra (see, for example, Refs. 70–75 and the references in them). Our approach to the description of hypernuclear states with the lowest  $0\hbar\omega$  configuration  $(p^{-1}s_\Lambda)$  is, in view of their manifest “purity” with respect to the center-of-mass motion, identical to the approach in the studies just cited. Significant differences arise when the decay properties of excited states, to which other configurations correspond, are considered (see Sec. 2 below).

## 2. FORMAL THEORY OF THE STRUCTURE OF $1p$ -SHELL HYPERNUCLEI

### Wave functions of hypernuclei in the TISM

When the wave functions of nuclei or hypernuclei are constructed in the shell model, the problem arises of separating the center-of-mass motion of the complete system. The concept of a state “pure” with respect to the center of mass means that the center of mass of the system executes vibrations with any integral value of the oscillator quanta and possesses energy  $(n + 3/2)\hbar\omega$ . The value  $n=0$  of the principal quantum number corresponds to the *zero-point vibrations*. It is well known from the theory of ordinary nuclei that if in addition to closed shells there is just one valence shell, then the center of mass executes zero-point vibrations. If there are two or more shells that are not closed, then in the general case “pure” states do not correspond to such configurations. Such a situation arises already for the  $1\hbar\omega$  excitation band.

The problem of classifying and constructing the wave functions of nuclear systems that correspond to zero-point or higher vibrations of the center of mass has been rigorously solved in the case when single-particle radial harmonic-oscillator functions are used. For hypernuclei, this problem can also be solved if it is assumed that the hyperon moves in the same oscillator well as the nucleons, i.e.,  $\hbar\omega_\Lambda = \hbar\omega_N$ . It is known that in the complete SSM basis of all states of the  $n\hbar\omega$  excitation band quite definite linear combinations of the basis functions correspond to pure states (excitation of the center of mass with given  $n \geq 0$ ). If TISM wave functions are given for a system of nucleons, one can find pure linear combinations of the SSM wave functions for excited states of the hypernucleus. A clear example illustrating manifestation of this type of *kinematic correlations* in hypernuclear wave functions is provided by excited hypernuclear states constructed on nuclear states with a hole in the valence shell [see Eq. (11)].

In our consideration of hypernuclear structure in the TISM, our point of departure will be the SSM, the formalism of which has been worked out in detail. Starting from this formalism, we obtain all the relations needed for the TISM. However, before we turn to hypernuclei, we recall briefly how the two models are related in the case of ordinary nuclei.

As we have already said, if only a valence shell is not closed, then the states corresponding to such a configuration are “pure,” and the center of mass executes zero-point vibrations. In such a case, the connection between the SSM and TISM functions is very simple. Let

$$|^4Z;e\rangle \equiv \{EJT\} = |s^4p^k;e\rangle \quad (1)$$

be the wave function of the nuclear system in the SSM in the intermediate-coupling scheme, or, in more expanded form,

$$|s^4p^k;e\rangle = \sum_{fLS} a_{fLS}^e |s^4p^k[f]LS:JT\rangle. \quad (2)$$

Here,  $a_{fLS}^{EJT} = a_{fLS}^e$  are the mixing coefficients due to the residual nucleon–nucleon interaction;  $S$ ,  $L$ , and  $J$  are the spin, orbital, and total angular momenta;  $f$  is the quantum number that characterizes the permutational symmetry of the state (Young diagram). Since the center of mass of a system with such a configuration executes zero-point vibrations, we can write (1) in the form

$$|s^4p^k;e\rangle = \Psi_{00}(\mathbf{R}_A) \Phi_k^A(\{\xi_A\};e). \quad (3)$$

The function  $\Psi_{00}(\mathbf{R}_A)$  describes the zero-point vibrations of the center of mass;  $\mathbf{R}_A$  is its radius vector;  $\{\xi_A\}$  is the set of Jacobi coordinates:

$$\begin{aligned} \mathbf{R}_A &= A^{-1} \sum_{i=1}^A \mathbf{r}_i \\ \xi_{1,2} &= \mathbf{r}_1 - \mathbf{r}_2, \\ \xi_{2,3} &= \mathbf{R}_2 - \mathbf{r}_3, \dots, \xi_{i,i+1} \\ &= \mathbf{R}_i - \mathbf{r}_{i+1}, \dots, \xi_{A-1,A} = \mathbf{R}_{A-1} - \mathbf{R}_A, \end{aligned} \quad (4)$$

where  $\mathbf{R}_i = i^{-1} \sum_{k=1}^i \mathbf{r}_k$ , in which  $\mathbf{r}_i$  are radius vectors of the individual particles. The internal function of the nucleus (the TISM function), which depends on the Jacobi coordinates, is defined as

$$\Phi_k^A(\{\xi_A\};e) = \frac{1}{\Psi_{00}(\mathbf{R}_A)} |s^4p^k;e\rangle. \quad (5)$$

If the residual hyperon–nucleon interaction is switched off, the hypernuclear internal wave function  $\Phi_{k+n}^{A+1}(\{\xi_A\}, \xi_{A,\Lambda}; e, j; \mathcal{M})$  (the TISM function) can be represented as a product of the internal wave function of the nuclear core (5) and the function  $\varphi_{nl}$  which describes the motion of the hyperon relative to the center of mass of the nucleus:

$$\begin{aligned} \Phi_{k+n}^{A+1}(\{\xi_A\}, \xi_{A,\Lambda}; e, j; \mathcal{M}) &= [\Phi_k^A(\{\xi_A\}; e(J)) \varphi_{nl}(\xi_{A,\Lambda} = \mathbf{R}_A - \mathbf{r}_{\Lambda}; j)]_{\mathcal{M}} \\ &= \sum \langle JMjm | \mathcal{M} \rangle \Phi_k^A(\{\xi_A\}; e(JM)) \varphi_{nl}(\xi_{A,\Lambda}; jm). \end{aligned} \quad (6)$$

The system of such functions has become known as the *weak-binding basis*.

We multiply the wave function (6) by  $\Psi_{00}(\mathbf{R}_{A+\Lambda})$  and denote it by

$$\begin{aligned} |_{\Lambda}^{A+1}Z;e,l,j;\mathcal{M}\rangle &= \Psi_{00}[(A\mathbf{R}_A + \mu\mathbf{r}_{\Lambda})/(A + \mu)] \\ &\times [\Phi_k^A(\{\xi_A\}; e(J)) \varphi_{nl}(\xi_{A,\Lambda}; j)]_{\mathcal{M}}. \end{aligned} \quad (7)$$

In (7),  $\mu = m_{\Lambda}/m_N$  is the ratio of the hyperon and nucleon masses. The Talmi–Moshinsky–Smirnov (TMS) transformation<sup>56,76</sup> then makes it possible to go over in (7) from the product of oscillator functions dependent on the coordinates  $\mathbf{R}_{A+\Lambda}$  and  $\xi_{A,\Lambda}$  to a product of functions that depend on the coordinates  $\mathbf{R}_A$  and  $\mathbf{r}_{\Lambda}$ :

$$\begin{aligned} \Psi_{00}(\mathbf{R}_{A+\Lambda}) \varphi_{nlm}(\xi_{A,\Lambda}) &= \sum_{\nu=0}^n \langle 00, n, l; l | A, \mu | N, L, \nu, l; l \rangle \\ &\times [\Psi_{NL}(\mathbf{R}_A) \Psi_{\nu l}(\mathbf{r}_{\Lambda})]_{lm}, \end{aligned} \quad (8)$$

where  $A = k + 4$  is the number of particles in the nuclear core;  $N + \nu = n$ ;  $L + l = l$ . The TMS coefficients in (8) do not depend on the quantum numbers of the internal motion of the nuclear core.

We shall call the expression

$$\begin{aligned} |_{\Lambda}^{A+1}Z;e,l,j;\mathcal{M}\rangle &= \left[ \Phi_k^A(\{\xi_A\}; e(J)) \sum_{\nu=0}^n \langle 00, n, l; l | A, \mu | N, L, \nu, l; l \rangle \right. \\ &\times \left. [\Psi_{NL}(\mathbf{R}_A) \Psi_{\nu l}(\mathbf{r}_{\Lambda})] \chi_{1/2}(\Lambda) \right]_{\mathcal{M}} \end{aligned} \quad (9)$$

the *wave function of the generalized SSM basis for the hypernucleus*. In (9),  $\chi_{1/2}(\Lambda)$  is the spin function of the  $\Lambda$  hyperon.

If the hyperon is in the lowest orbit, then  $n = l = 0$ , and in (9) there remains only the term with  $N = \nu = 0$ . At the same time, the TMS coefficient is equal to unity, and we obtain the ordinary weak-binding function of the SSM:

$$\begin{aligned} \Psi_{00}(\mathbf{R}_{A+\Lambda}) \varphi_{00}(\xi_{A,\Lambda}) [\Phi_k^A(\{\xi_A\}; e(J)) \chi_{1/2}(\Lambda)]_{\mathcal{M}} &= [\Psi_{00}(\mathbf{R}_A) \Phi_k^A(\{\xi_A\}; e(J)) \varphi_{00}(\mathbf{r}_{\Lambda}) \chi_{1/2}(\Lambda)]_{\mathcal{M}} \\ &= [|^4Z; e(J)\rangle \Psi_{00}(\mathbf{r}_{\Lambda}) \chi_{1/2}(\Lambda)]_{\mathcal{M}}. \end{aligned} \quad (10)$$

For  $n > 0$ , the expression (9) will contain both the zero-point and higher vibrations of the center of mass of the core nucleus. For  $(p^{-1}p_{\Lambda})$  states with  $n = l = 1$ , we obtain from (9) a superposition of SSM states with zero-point vibration of the center of mass of the hypernucleus:

$$\begin{aligned} \Psi_{00}(\mathbf{R}_{A+\Lambda}) \Phi_{k+1}^{A+1}(\{\xi_A\}, \xi_{A,\Lambda}; e(J), 1p, j; \mathcal{M}) &= \Psi_{00}(\mathbf{R}_{A+\Lambda}) [\Phi_k^A(\{\xi_A\}; e(J)) \varphi_{11}(\xi_{A,\Lambda}; j)]_{\mathcal{M}} \\ &= \alpha [\Phi_k^A(e, J) \Psi_{00}(\mathbf{R}_A) [\Psi_{11}(\mathbf{r}_{\Lambda}) \chi_{1/2}(\Lambda)]_j]_{\mathcal{M}} \\ &\quad + \beta [\Phi_k^A(e, J) [\Psi_{11}(\mathbf{R}_A) \chi_{1/2}(\Lambda)]_j \Psi_{00}(\mathbf{r}_{\Lambda})]_{\mathcal{M}}, \end{aligned} \quad (11)$$

where  $\alpha = [A/(A + \mu)]^{1/2}$ ,  $\beta = -[\mu/(A + \mu)]^{1/2}$ . For each level with  $(p^{-1}p_{\Lambda})$  configuration we can obtain in the same manner a “spurious” state that is orthogonal to (11), corresponds to  $1\hbar\omega$  excitation of the center of mass of the hypernucleus, and is obtained by the substitution  $\alpha \rightarrow -\beta$ ,  $\beta \rightarrow -\alpha$  on the right-hand side of (11). Note that the function (11) contains all the SSM  $1\hbar\omega$  states:  $(p^{-1}p_{\Lambda})$ ,  $(s^{-1}s_{\Lambda})$ , and  $(p^{-2}l_{\Lambda})$ . Here, we shall not construct the TISM wave functions; for our purposes, it is entirely sufficient to use a fractional-parentage expansion

of the TISM wave function of the system of  $A$  particles with respect to the wave functions of  $A - 1$  or a smaller number of particles and to know how to relate the resulting coefficients of fractional parentage (CFP) to the corresponding CFP in the SSM.

In shell-model calculations, the CFP play the part of basic structural units, by means of which the many-particle problem is reduced to a two- or three-body problem. The method of calculating these coefficients in the standard shell model is well developed.

### Fractional-parentage expansion of hypernuclear wave functions in the TISM

The fractional-parentage expansion of the hypernuclear function  $|^{A+1}Z\rangle$  with respect to the functions of the nuclear core  $|^AZ\rangle$  and the hyperon is obvious—because the nucleon and hyperon are not identical, the corresponding CFP is simply equal to unity [see the expression (6)].

In hypernuclear spectroscopy, problems arise when in the hypernuclear wave function it is necessary to make a fractional-parentage separation, not of the hyperon, but of a nucleon or a group of baryons—a nucleon association or a light hyperfragment. In the first place, we are referring here to problems of decay of hypernuclear states through the nucleonic channel, and also with the emission of the lightest nuclei  ${}^2,3\text{H}$ ,  ${}^3,4\text{He}$  and hypernuclei  ${}^3,4\text{H}$  and  ${}^4,5\text{He}$ . In addition, a fractional-parentage expansion with separation of a nucleon is, of course, necessary in calculations of the matrix elements of the residual  $\Lambda N$  interaction; for these occur in the energy matrices whose diagonalization gives the spectrum and wave functions of the hypernucleus.

The method that will be used to obtain the CFP is the same as in the SSM; first, a nucleon is separated from any internal shell, and then the recoupling of the angular momenta needed for subsequent transformations is carried out. A transition is then made to a different set of Jacobi variables with additional recoupling of the angular momenta, this ensuring that the hyperon is joined to the core nucleus. As we shall show, this procedure reveals the *kinematic correlations of baryons* existing in the many-particle system. Because of the complexity of the expressions for the CFP for separation of nucleon associations for separation of nucleon associations and hyperfragments, they will not be given here, although the computational scheme for obtaining them is the same.

We show first how to obtain the CFP for separation of a nucleon from a nuclear valence shell, when the connection between the CFP in the TISM and in the SSM is particularly simple.

### Coefficients of fractional parentage for separation of a nucleon in the nuclear wave function

The TISM coefficient of fractional parentage  $g_{E'JT}^{EJT}(nlj) \equiv g_e^e(nlj)$  for separation of a nucleon with quantum numbers  $nlj$  in the wave function of  $A$  nucleons is determined in complete analogy with the CFP in the SSM as the corresponding coefficient of the fractional-parentage

expansion of this state with respect to all wave functions of the system of  $A - 1$  nucleons:

$$\begin{aligned} \Phi_k^A(\{\xi_A\}; e) &= \sum_{nlj} \sum_{e'} g_e^e(nlj) \\ &\times [\Phi_{k-n}^{A-1}(\{\xi_c\}; e') \varphi_{nl}(\xi_{c,n} \\ &= \mathbf{R}_c - \mathbf{r}_j)]_{JM}. \end{aligned} \quad (12)$$

It is clear from (12) that the CFP is the matrix element

$$g_e^e(nlj) = \langle \Phi_k^A(\{\xi_A\}; e), [\Phi_{k-n}^{A-1}(\{\xi_c\}; e') \varphi_{nl}(\xi_{c,n})]_J \rangle. \quad (13)$$

As we noted above, particular attention will be devoted to the hypernuclear configurations  $|s^4 p^k e, n_{\Lambda} l_{\Lambda} j_{\Lambda} \mathcal{F} \mathcal{M}\rangle$ , and we actually need only the CFP  $g_e^e(1pj)$  for separation of a nucleon from the valence  $1p$  shell. One can show that in this case the CFP in the TISM is very simply related to the CFP in the SSM:

$$\begin{aligned} g_e^e(1pj) &= \left( \frac{k+4}{k+3} \right)^{1/2} \sum_{\alpha, \alpha'} a_{\alpha}^e b_{\alpha'}^{e'} \begin{vmatrix} L' & 1 & L \\ S' & 1/2 & S \\ J' & j & J \end{vmatrix} \\ &\times \langle s^4 p^k \alpha T | s^4 p^{k-1} \alpha' T', p \rangle. \end{aligned} \quad (14)$$

In (14),  $a_{\alpha}^e = a_{fLS}^{EJT}$  and  $b_{\alpha'}^{e'} = b_{f'L'S'}^{E'JT'}$  are the coefficients of the expansion of the wave functions  $\Phi_k^A$  and  $\Phi_{k-1}^{A-1}$  with respect to the basis functions in  $LS$  coupling; the  $9j$  symbol (Racah's definition<sup>77</sup>) which occurs in (14) ensures the necessary recoupling of the angular momenta; by definition, the coefficient

$$\langle s^4 p^k \alpha T | s^4 p^{k-1} \alpha' T', p \rangle = \left( \frac{k}{k+4} \right)^{1/2} \langle p^k \alpha T | p^{k-1} \alpha' T', p \rangle \quad (15)$$

is the CFP for separation of the  $1p$  nucleon in the SSM; the factor  $[(k+4)/(k+3)]^{1/2}$  in (14) is obtained as a result of separation of the center-of-mass system.<sup>56</sup>

We shall not give here the standard calculations; we merely mention that the relation (14) is obtained if in the matrix element (13) we go over from the TISM functions to the functions in the SSM by substituting in the integral the square of the center-of-mass zero-point vibration function  $\Psi_{00}(\mathbf{R}_A)$ , introducing an additional integration with respect to the variable  $\mathbf{R}_A$ , and using the TMS coefficients in the product transformation  $\Psi_{00}(\mathbf{R}_A) \varphi_{nl}(\xi_{c,n}) \rightarrow \Psi_{00}(\mathbf{R}_{A-1}) \Psi_{nl}(\mathbf{r})$ .

Note that the CFP (14) do not depend on the choice of the particular basis. For nuclear ground-state functions, the CFP determine the *spectroscopic factors*  $S$ , which are the subject of experimental study in the pickup reactions  $(p, 2p)$ ,  $(p, pn)$ , and  $(e, e'p)$ .<sup>2)</sup>

$$C^2 S(e', j) = \langle T' T_z' \frac{1}{2} \tau_z | T T_z \rangle^2 \{g_e^e(nlj)\}^2. \quad (16)$$

The CFP for excited states occur in the definition of transition densities. We now turn to the fractional-parentage



expansion of the hypernuclear function (6) of the translationally invariant shell model.

### Recoupling of the angular momenta of the core nucleus, nucleon, and hyperon

We substitute the expansion (12) in (6), introduce the total angular momentum of the nucleon-hyperon pair,  $I = j + j_\Lambda$ , and write the function of this pair in  $LS$  coupling. After the appropriate transformations, the hypernuclear wave function (6) takes the form

$$\begin{aligned} & \Phi_{k+n_\Lambda}^{A+1}(\{\xi_A\}, \xi_{A,\Lambda}; e, j_\Lambda; \mathcal{J} \mathcal{M}) \\ &= \sum_{nlj} \sum_{LSI} g_{e'}^{nlj} U(J' j j_\Lambda; J I) \begin{vmatrix} l & 1/2 & j \\ l_\Lambda & 1/2 & j_\Lambda \\ L & S & I \end{vmatrix} \\ & \times [\Phi_{k-n}^{A-1}(\{\xi_c\}, e')] \\ & \times [\varphi_{nl}(\xi_{c,nj}) \varphi_{n_\Lambda \Lambda}(\xi_{A,\Lambda j})]_{LSI} \mathcal{J} \mathcal{M}. \end{aligned} \quad (17)$$

In the relation (17), the Racah coefficient  $U$  takes into account the recoupling of the intermediate angular momenta in the three-body system consisting of the core nucleus ( $J'$ ), which itself consists of  $A-2$  nucleons, the nucleon ( $j$ ), and the hyperon ( $j_\Lambda$ ), subject to the condition  $J' + j + j_\Lambda = J$ . The separated nucleon was initially coupled to the core nucleus ( $J' + j = J$ ), while on the right-hand side of (17) it is coupled to the hyperon ( $j + j_\Lambda = I$ ).

### Transition to new Jacobi variables

The expression for the hypernuclear wave function (6) in the form (17) actually amounts to transition from its two-body representation in terms of a nucleus and a hyperon (Jacobi variables  $\{\xi_A\}$  and  $\{\xi_{A,\Lambda}\}$ ) to the three-body representation in terms of the core nucleus of  $A-2$  nucleons, a nucleon, and the hyperon (Jacobi variables  $\{\xi_c\}$ ,  $\xi_{c,n}$ , and  $\xi_{A,\Lambda}$ ).

The further course of the solution of the problem to determine the CFP for separation of the nucleon with formation of the hypernucleus  $^{A-2}_\Lambda Z$  or calculation of the two-particle matrix elements of the  $\Lambda N$  interaction requires transition in (17) to other Jacobi variables.

In the three-body system consisting of the core nucleus, nucleon, and hyperon, which have radius vectors  $\mathbf{R}_c$ ,  $\mathbf{r}_n$ , and  $\mathbf{r}_\Lambda$  and masses  $m_c = (A-1)m$ ,  $m_\Lambda = \mu m$  ( $m$  is the nucleon mass), it is possible to introduce three pairs of independent Jacobi variables:

$$\begin{aligned} \xi_{A,\Lambda} &= \mathbf{R}_A - \mathbf{r}_\Lambda; \\ \xi_{c,n} &= \mathbf{R}_c - \mathbf{r}_n; \end{aligned} \quad (18a)$$

$$\begin{aligned} \xi_{c,n+\Lambda} &= \mathbf{R}_c - (\mathbf{r}_n + \mu \mathbf{r}_\Lambda) / (1 + \mu); \\ \xi_{n,\Lambda} &= \mathbf{r}_n - \mathbf{r}_\Lambda; \end{aligned} \quad (18b)$$

$$\begin{aligned} \xi_{c+\Lambda,n} &= ((A-1)\mathbf{R}_c + \mu \mathbf{r}_\Lambda) / (A-1+\mu) - \mathbf{r}_n; \\ \xi_{c,\Lambda} &= \mathbf{R}_c - \mathbf{r}_\Lambda. \end{aligned} \quad (18c)$$

Further, in order to use the well-known Talmi-Moshinsky-Smirnov transformation for the nucleon and hyperon wave functions, it is necessary to go over in (17) to dimensionless Jacobi variables. For this, we introduce the ratios of all the radius vectors in (18a)–(18c) to the oscillator parameters  $r_{0i} = (\hbar/\mu_i \omega)^{1/2}$  corresponding to them. The dimensionless variables corresponding to the sets (18a)–(18c) obtained in this manner are written in the same order as

$$\mathbf{x}_1 = \sqrt{\frac{(A-1)\mu}{(A+\mu)A}} \mathbf{R}'_c + \sqrt{\frac{\mu}{(A+\mu)A}} \mathbf{r}'_n - \sqrt{\frac{A}{A+\mu}} \mathbf{r}'_\Lambda; \quad (19a)$$

$$\begin{aligned} \mathbf{y}_1 &= \sqrt{\frac{1}{A}} \mathbf{R}'_c - \sqrt{\frac{A-1}{A}} \mathbf{r}'_n; \\ \mathbf{x}_2 &= \sqrt{\frac{1+\mu}{A+\mu}} \mathbf{R}'_c - \sqrt{\frac{A-1}{(A+\mu)(1+\mu)}} \mathbf{r}'_n \\ &+ \sqrt{\frac{\mu(A-1)}{(A+\mu)(1+\mu)}} \mathbf{r}'_\Lambda; \end{aligned} \quad (19b)$$

$$\begin{aligned} \mathbf{y}_2 &= \sqrt{\frac{\mu}{1+\mu}} \mathbf{r}'_n - \sqrt{\frac{1}{1+\mu}} \mathbf{r}'_\Lambda; \\ \mathbf{x}_3 &= \sqrt{\frac{A-1}{(A+\mu)(A+\mu-1)}} \mathbf{R}'_c \\ &+ \sqrt{\frac{\mu}{(A+\mu)(A+\mu-1)}} \mathbf{r}'_\Lambda - \sqrt{\frac{A+\mu-1}{A+\mu}} \mathbf{r}'_n; \end{aligned} \quad (19c)$$

$$\mathbf{y}_3 = \sqrt{\frac{\mu}{A+\mu-1}} \mathbf{R}'_c - \sqrt{\frac{A-1}{A-1+\mu}} \mathbf{r}'_\Lambda,$$

where  $\mathbf{R}'_c = \mathbf{R}_c/r_{0c}$ ,  $\mathbf{r}'_n = \mathbf{r}_n/r_{0n}$ ,  $\mathbf{r}'_\Lambda = \mathbf{r}_\Lambda/r_{0\Lambda}$ .

The pairs of vectors  $(\mathbf{x}_i, \mathbf{y}_i)$  are related by the unitary transformation

$$\begin{pmatrix} \mathbf{x}_i \\ \mathbf{y}_i \end{pmatrix} = \begin{pmatrix} \alpha_{ik} & \beta_{ik} \\ \beta_{ik} & -\alpha_{ik} \end{pmatrix} \begin{pmatrix} \mathbf{x}_k \\ \mathbf{y}_k \end{pmatrix}. \quad (20)$$

To calculate the matrix elements of the residual  $\Lambda N$  interaction, we need the coefficients

$$\alpha_{12} = \sqrt{\frac{\mu(A-1)}{A(1+\mu)}}; \quad \beta_{12} = \sqrt{\frac{A+\mu}{A(1-\mu)}}, \quad (21a)$$

and to determine the single-nucleon CFP, the coefficients

$$\alpha_{13} = -\sqrt{\frac{\mu}{A(A+\mu-1)}}; \quad \beta_{13} = \sqrt{\frac{(A+\mu)(A-1)}{A(A+\mu-1)}}. \quad (21b)$$

The oscillator functions of the nucleon and hyperon in (17) can, after the transformation (20) with allowance for (21a) [or (21b)], be expressed in terms of the Talmi-Moshinsky-Smirnov coefficients and the product of oscillator functions of the new variables:

$$[\varphi_{nl}(\mathbf{y}_1) \varphi_{n_\Lambda \Lambda}(\mathbf{x}_1)]_L = \sum \langle nl, n_\Lambda l_\Lambda; L | \alpha^2 \beta^2 | \nu \lambda, n' l'; L \rangle$$

$$\times [\varphi_{\nu\lambda}(\mathbf{y}_i) \varphi_{n'l'}(\mathbf{x}_i)]_L. \quad (22)$$

Note that the transformation (22), for given initial quantum numbers of the nucleon separated from the core nucleus,  $(n, l)$ , and of the hyperon,  $(n_\Lambda, l_\Lambda)$ , leads to different excitations  $(n', l')$  of the nucleon distinguished in the total hypernuclear function, and also to different excitations  $(\nu, \lambda)$  of the hyperon, which forms together with the  $A - 2$  nucleons of the core nucleus the hyperfragment  ${}^{A-1}_\Lambda \mathbf{Z}$ . This is a manifestation of the *kinematic correlations of the baryons* in the wave function of the hypernuclear resonance, which play an important part in the study of decays with emission of nucleons.

### Recoupling of angular momenta with "attachment" of a hyperon to a core nucleus

The "attachment" of the hyperon to the  $A - 2$  nucleons of the core nucleus is achieved by substituting (22) in (17) and subsequent vector coupling of the functions of the nucleus with quantum numbers  $e' \equiv \{E' J' T'\}$  and of the hyperon with angular momentum  $j_\Lambda$ . Omitting the tedious calculations, we finally obtain for the single-nucleon fractional-parentage expansion of the function (17) the expression

$$\begin{aligned} \Phi_{k+n_\Lambda}^{A+1}(\{\xi_A\}, \xi_{A,\Lambda}; e; j_\Lambda; \mathcal{J} \mathcal{M}) \\ = \sum_{n'l'j'} \sum_{e'j'_\Lambda} G_{e'j'_\Lambda}^{ej_\Lambda \mathcal{J}}(n'l'j') \\ \times [ [\Phi_k^{A-1}(\{\xi_c\}, e') \varphi_{\nu\lambda}(\xi_{c,\Lambda}; j'_\Lambda) ]_{\mathcal{J}'} \\ \times \varphi_{n'l'}(\xi_{c+\Lambda, n'l'}) ]_{\mathcal{J} \mathcal{M}}, \end{aligned} \quad (23)$$

where  $e', j'_\Lambda, \mathcal{J}'$  are the quantum numbers of the residual hypernucleus.

It is natural to call the coefficient  $G_{e'j'_\Lambda}^{ej_\Lambda \mathcal{J}}(n'l'j')$  in (23) the CFP for separation of a nucleon in the hypernuclear wave function. It can be expressed as a product of three factors:

$$\begin{aligned} G_{e'j'_\Lambda}^{ej_\Lambda \mathcal{J}}(n'l'j') = g_e^e(nl_j) Z_{j'_\Lambda}^{jj_\Lambda}(J' J \mathcal{J}' \mathcal{J}) \\ \times \langle n l, n_\Lambda l_\Lambda; L | \alpha^2 / \beta^2 | \nu \lambda, n' l'; L \rangle. \end{aligned} \quad (24)$$

In (24), the first factor ( $g$ ) is the CFP for separation of a nucleon from the core nucleus; the second, which is a sum of products of  $6j$  and  $9j$  symbols and is equal to

$$\begin{aligned} Z_{j'_\Lambda}^{jj_\Lambda}(J' J \mathcal{J}' \mathcal{J}) = \sum_{LSI} U(J' j \mathcal{J}' j_\Lambda; JI) \\ \times \begin{vmatrix} l & \frac{1}{2} & j \\ l_\Lambda & \frac{1}{2} & j_\Lambda \\ L & S & I \end{vmatrix} \begin{vmatrix} \lambda & \frac{1}{2} & j'_\Lambda \\ l' & \frac{1}{2} & j' \\ L & S & I \end{vmatrix} \\ \times U(J' j'_\Lambda \mathcal{J}' j'; \mathcal{J}' I), \end{aligned} \quad (25)$$

takes into account the recoupling of the angular momenta; the third factor is associated with the transformation of the product of functions (22).

To conclude this section, we mention the most important consequences that flow from the solution of the problem of separating a nucleon in the hypernuclear functions of the TISM. As we noted in Sec. 1, a specific feature of excited hypernuclear states is that the states with configuration  $(p^{-1} p_\Lambda)$  are energetically separated from the  $(s^{-1} s_\Lambda)$  states, and in the solution of many problems it is sensible to consider only the  $(p^{-1} p_\Lambda)$  excitations. In this case, the transformations (22) and (23) are needed to describe decays with emission of nucleons. In separating one nucleon and then forming the hypernucleus-core system [see the relation (23)], we effectively rearrange the orbitals of the hyperon ( $n_\Lambda l_\Lambda \rightarrow \nu \lambda$ ) and the nucleon ( $nl \rightarrow n'l'$ ). What is of practical interest in such a transformation of the basis functions is the possibility that it opens up of obtaining, in the expansion (23) of the  $0\hbar\omega$  band, states of the hypernucleus-core system with the hyperon in the  $0s$  shell ( $\nu = \lambda = 0$ ), while the nucleon separated from the  $1p$  shell of the core nucleus automatically goes into higher unoccupied orbitals with  $n' = 2$  ( $l' = 0$  and  $2$ ). This feature of the single-nucleon expansion of the hypernuclear function (23), which reflects the kinematic correlations of the baryons in the TISM, makes it possible to calculate the probabilities of decay of  $1\hbar\omega$  resonances with configuration  $(p^{-1} p_\Lambda)$  through the nucleonic channel with population of low-lying levels of the daughter hypernuclei. The corresponding spectroscopic amplitudes of nucleonic decay are determined by the CFP (24) of the translationally invariant shell model.

The formalism presented here of the rearrangement of the baryon  $(p^{-1} p_\Lambda)$  and  $(p^{-2} l s_\Lambda)$  orbits in the TISM explicitly introduces the kinematic correlations of the baryons that are present in the many-particle system with the center-of-mass motion eliminated. Thus, the TISM gives the key to the most economic way of taking into account the  $(p^{-2} l s_\Lambda)$  states; in contrast to the standard shell model, it does not require an excessively cumbersome procedure for including for this purpose all  $1\hbar\omega$  basis shell states of the hypernucleus in the computational scheme.

Detailed study of the decay properties of the  $1\hbar\omega$  excitations in hypernuclei is deferred to the second part of the review.

### Intermediate coupling in hypernuclei and hyperon-nucleon forces

The wave function of the hypernucleus can be expressed like (2) as a linear combination of the basis functions (7):

$$\begin{aligned} |{}^{A+1}_\Lambda \mathbf{Z}(\xi \mathcal{J} T)\rangle = \Psi_{00}(\mathbf{R}_{A+\Lambda}) \sum_{ij_\Lambda} a_e^e(nl j_\Lambda) \\ \times [\Phi_k^A(\{\xi_A\}; e) \varphi_{nl}(\xi_{A,\Lambda}; j_\Lambda) ]_{\mathcal{J} \mathcal{M}}. \end{aligned} \quad (26)$$

In the expansion (26), the coefficients  $a_e^e(nl j_\Lambda) = a_{EJT}^{e \mathcal{J} T}(nl j_\Lambda)$ , which determine the wave functions in the

intermediate coupling, are obtained together with the energy eigenvalues by the diagonalization of the energy matrices:

$$\begin{aligned} H_{e\Lambda, \bar{e}\Lambda}^{\mathcal{J}} &= \langle s^4 p^k; e j_{\Lambda}; \mathcal{J} | H | s^4 p^k; \bar{e} \bar{j}_{\Lambda}; \mathcal{J} \rangle \\ &= E(JT) \delta_{e, \bar{e}} + \varepsilon_{nl} \Delta_{j_{\Lambda} \bar{j}_{\Lambda}} \\ &\quad + \langle s^4 p^k; e j_{\Lambda}; \mathcal{J} | V | s^4 p^k; \bar{e} \bar{j}_{\Lambda}; \mathcal{J} \rangle, \end{aligned} \quad (27)$$

where  $E(JT)$  is the excitation energy of the core nucleus, and  $\varepsilon_{nl}$  is the single-particle energy of the hyperon in the field of the nucleus. The two-particle matrix elements of the residual  $\Lambda N$  interaction  $V = V_{\Lambda N} - V_0$  ( $V_0$  is the mean field for the hyperon in the nucleus) can be calculated by means of the technique of coefficients of fractional parentage described above:

$$\begin{aligned} &\langle s^4 p^k; e j_{\Lambda}; \mathcal{J} | V | s^4 p^k; \bar{e} \bar{j}_{\Lambda}; \mathcal{J} \rangle \\ &= (k+4) \sum_I \sum_{LS, \bar{L}\bar{S}} \left\{ \sum_{e'} G_{e'}^{ej_{\Lambda}\mathcal{J}}(LSI) G_{e'}^{\bar{e}\bar{j}_{\Lambda}\mathcal{J}}(\bar{L}\bar{S}I) \right\} \\ &\quad \times \langle pl: LSI | V | pl: \bar{L}\bar{S}I \rangle. \end{aligned} \quad (28)$$

In (28),  $G_{e'}^{ej_{\Lambda}\mathcal{J}}(LSI)$  is the coefficient of fractional parentage for separation of a  $\Lambda N$  pair with quantum numbers  $LSI$ :

$$\begin{aligned} G_{e'}^{ej_{\Lambda}\mathcal{J}}(LSI) &= \langle s^4 p^k; e j_{\Lambda}; \mathcal{J} | s^4 p^{k-1}; e', pl(LSI); \mathcal{J} \rangle \\ &= \sum_{j_n} g_{e'}^e(j_n) U(J' j_n \mathcal{J} j_{\Lambda} JI) \begin{vmatrix} 1 & \frac{1}{2} & j_n \\ e & \frac{1}{2} & j_{\Lambda} \\ L & S & I \end{vmatrix}. \end{aligned} \quad (29)$$

Since the number of matrix elements  $\langle pl: LSI | V | pl: \bar{L}\bar{S}I \rangle$  is usually small, while the number of excited states of a given band of  $n\hbar\omega$  excitations for all  $1p$ -shell hypernuclei is large, it is convenient to regard these matrix elements as parameters. They can be determined either from the spectra of excited states, or calculated using realistic potentials  $V$ . Such methods of determining the matrix elements of the  $NN$  interaction have long been used in nuclear physics, in which there are, besides the nuclear spectra, many data on  $NN$  scattering phase shifts and some global characteristics of nuclear matter. As a result of many investigations, it has been established that features of nuclear interactions such as the repulsion at short distances or the many-particle forces mainly influence the binding energy and compressibility of nuclei. In contrast, the energy spectra of nuclei are basically sensitive to the spin (and exchange) dependence of the two-particle  $NN$  potentials, which include central, spin-orbit, and tensor components.

Information about the free  $\Lambda N$  interaction is very limited,<sup>78</sup> and therefore hyperon-nucleon potentials are most often obtained by analogy with nucleon-nucleon potentials by using elements of meson theory.<sup>79</sup> An important feature of  $\Lambda N$  interactions is the absence of a contribution of one-pion exchange, which is the main part of the poten-

tial of the  $\Lambda N$  interaction. The  $\Lambda N$  forces therefore have a shorter range and contain contributions of exchanges of two pions,  $K$  mesons, and other particles. Small components in the  $\Lambda N$  potential that break the charge symmetry can arise from the breaking of the isospin symmetry for  $\Lambda$  and  $\Sigma$  hyperons and some mesons.<sup>80</sup> These effects are manifested in the binding energies of the  $\Lambda$  hyperon in  ${}^4\text{H}$  and  ${}^4\text{He}$  (Ref. 44). A contribution to the interaction of the  $\Lambda$  hyperon with the nucleons can also be made by three-particle  $\Lambda NN$  forces (two-pion exchange, etc.), but as yet no clear effects in which they are manifested have been found. It is possible that they influence the  $A$  dependence of the single-particle energies of the  $\Lambda$  hyperon.<sup>81</sup>

At the present time, hypernuclei are the main source of information about the  $\Lambda A$  and  $\Lambda N$  interactions at low energies. When information about these interactions is deduced, it is important to take into account correctly the influence of the structure of the many-particle system. One of the methods of taking into account the structure factors is the procedure for extracting the parameters of the residual  $\Lambda N$  forces in the shell model, which has proved itself well in an analysis of the spectra of ordinary nuclei. In the early stage of development, the shell model was used mainly to analyze the binding energies  $B_{\Lambda}$  of the  $\Lambda$  hyperon, although it is precisely the description of the binding energies that is one of the weakest aspects of this model (see Sec. 4). Despite this, important results have been obtained in the most advanced form of the shell model (Refs. 38, 70–72, and 74), which is related in some degree to ideas about the hyperon-nucleon interaction in meson theory. These results offer the hope that the approach can be successfully used in hypernuclear spectroscopy as data are accumulated on the hypernuclear levels. We should like to consider some of these results obtained using the model of Refs. 70–72, since it is also used in our analysis of experimental data on hypernuclear  $\gamma$  transitions.

1. A parametrization of the  $\Lambda N$  interaction that is convenient from the physical point of view has been found for the  $0\hbar\omega$  band of excitations in the hypernuclei of the  $1p$  shell ( $\Lambda$  hyperon in the  $0s$  shell). Five matrix elements of the two-particle interaction,

$${}^{2S+1}\mathcal{P}_I = \langle ps_{\Lambda}; {}^{2S+1}P_I | V | ps_{\Lambda}; {}^{2S+1}P_I \rangle; \quad (30)$$

$$\mathcal{P} = \langle ps_{\Lambda}; {}^3P_1 | V | ps_{\Lambda}; {}^1P_1 \rangle,$$

are expressed as linear combinations of the parameters of  $V_{\alpha}$  ( $\bar{V}$ ,  $\Delta$ ,  $S_{\Lambda}$ ,  $S_N$ , and  $T$ ) corresponding to radial matrix elements of individual components of the  $\Lambda N$  potential:

$$\begin{aligned} V(r) &= V_0(r) + V_{\sigma}(r) \mathbf{S}_N \mathbf{S}_{\Lambda} + V_{\Lambda}(r) \mathbf{1}_{N\Lambda} S_{\Lambda} \\ &\quad + V_N(r) \mathbf{1}_{N\Lambda} S_N + V_T(r) S_{12} \\ (S_{12} &= 3(\boldsymbol{\sigma}_N \hat{\mathbf{r}})(\boldsymbol{\sigma}_{\Lambda} \hat{\mathbf{r}}) - \boldsymbol{\sigma}_N \boldsymbol{\sigma}_{\Lambda}). \end{aligned} \quad (31)$$

The structure of the potential (31), which contains central, spin-spin, spin-orbit, and tensor parts, is motivated by the consideration of various meson exchanges.

The explicit form of the matrix elements is

$${}^1\mathcal{P}_1 = \bar{V} + \frac{3}{4}\Delta;$$

$$\begin{aligned}
{}^3\mathcal{P}_0 &= \bar{V} - \frac{1}{4}\Delta + (S_N + S_\Lambda) + 6T; \\
{}^3\mathcal{P}_1 &= \bar{V} - \frac{1}{4}\Delta + \frac{1}{2}(S_\Lambda + S_N) - 3T; \\
{}^3\mathcal{P}_2 &= \bar{V} - \frac{1}{4}\Delta - \frac{1}{2}(S_\Lambda + S_N) + \frac{3}{2}T; \\
\mathcal{P} &= \frac{1}{\sqrt{2}}(S_\Lambda - S_N).
\end{aligned} \tag{32}$$

The parameter  $\bar{V}$  does not influence the splitting of the levels in the hypernucleus; it merely gives rise to a common shift of all levels of the configuration  $\{s^4 p^n \otimes s_\Lambda; \mathcal{J} T\}$ .

2. It has been established that for many low-lying hypernuclear states a weak coupling of the hyperon to the nuclear states is realized, and the position of the hypernuclear level depends linearly on the parameters  $V_\alpha$ :

$$\varepsilon(\mathcal{J}) = E(e) + \sum_{\alpha} D_{\alpha}^e(\mathcal{J}) V_{\alpha} \tag{33}$$

where the coefficients

$$D_{\alpha}^e(\mathcal{J}) = \sum_{IS} \left\{ \sum_{e'} G_{e'}^{\frac{1}{2}\mathcal{J}} (1SI) G_{e'}^{\frac{1}{2}\mathcal{J}} (1\bar{S}I) \right\} W_{\alpha}^{1S\bar{S}}, \tag{34}$$

which include the fractional-parentage separation of the  $\Lambda N$  pair, contain information about the structure of the core nuclear state. In (34),  $W_{\alpha}^{1S\bar{S}}$  is a matrix that in (32) relates the parameters (30) and  $V_{\alpha}$ . The relations (33) make it significantly easier to recover  $V_{\alpha}$  from experimental data on the energies of hypernuclear levels.

3. With the set of parameters  $\{V_{\alpha}\}$ , the splitting of the hypernuclear doublets  $\{\xi(\mathcal{J} = J \pm \frac{1}{2}), T\}$  constructed on a given nuclear state  $\{EJT\}$  depends only on three parameters:  $\Delta$ ,  $S_{\Lambda}$ , and  $T$ . The parameter  $S_{\Lambda}$  influences the positions of the doublets formed on different nuclear states. In rare cases, the splitting of a doublet depends on a single parameter  $V_{\alpha}$ . For example, the splitting of the hypernuclear doublet  ${}^4S_{3/2}$ ,  ${}^2S_{1/2}$  constructed on the nuclear state  ${}^3S_1$  (ground state of  ${}^6\text{Li}$ ) depends only on  $\Delta$ , and the splitting of the doublet  ${}^2D_{5/2}$ ,  ${}^2D_{3/2}$  constructed on the nuclear state  ${}^1D_2$  ( ${}^8\text{Be}$ ) is determined by  $S_{\Lambda}$ .

Thus, as will be seen from the subsequent exposition, the physically transparent parametrization (32) of the  $\Lambda N$  interaction makes it possible to obtain, from analysis of hypernuclear spectra, information about individual parts of the  $\Lambda N$  interaction.

### 3. OTHER METHODS IN THE THEORY OF HYPERNUCLEAR STRUCTURE

In nuclear theory, numerous models have been developed to describe a system of  $A$  particles. These models differ from each other in the first place in the choice of the properties studied (single-particle or collective) and also in the techniques used to solve the basic equations of the theory—the Hartree–Fock approach, variational method, cluster models, hyperspherical-function method, etc. Many of these approximations have been used to study the spectroscopic characteristics of individual hypernuclei and also the influence of the hyperon on the properties of the nucleon core.

It is attractive to use the translationally invariant shell model employed here in hypernuclear physics not only because of the universality of its simultaneous and systematic description of many aspects of the “birth, life, and death” of hypernuclei, i.e., the entire complex of interrelated problems of the formation, structure, and decays of hypernuclear states. Because the individual motion of all  $A$  particles forming the hypernucleus is taken into account at the microscopic level, the TISM is simultaneously a good basis for comparing different approaches. At the present stage of hypernuclear investigations, a particularly important role is played by target nuclei of the  $1p$  shell, in which the distances between the lowest nuclear levels are, as a rule, large, so that weak binding is applicable), and there is extensive spectroscopic information on hypernuclei and, especially, ordinary nuclei.<sup>82</sup>

In the weak-binding basis

$$|{}^A+1Z(\xi\mathcal{J}T)\rangle = |{}^AZ(EJT) \otimes j_{\Lambda}; \mathcal{J}T\rangle \tag{35}$$

one can readily establish the growth structure of the expected hypernuclear spectrum—the addition of a hyperon to a given orbit very often simply leads to a multiplet splitting of known nuclear levels with a slight mixing of the states (35). The splitting depends on the structure of the core nucleus and on the parameters of the residual  $\Lambda N$  interaction. Some excited states of hypernuclei, for example, those corresponding to the  $1\hbar\omega$  configuration  $|s^4 p^k, p_{\Lambda}\rangle$ , are sometimes more conveniently classified by means of the quantum numbers  $(\lambda\mu)$  of the group  $SU(3)$ :

$$|s^4 p^k [f_N] L_N S_N T_N p_{\Lambda} [f_1 f_2 f_3] (\lambda\mu) L S \mathcal{J}\rangle. \tag{36}$$

In such a classification, it is very simple to separate the “genuinely” hypernuclear states,<sup>53,63</sup> which possess an orbital symmetry  $(f_1 = 5)$  greater than that possible for ordinary nuclei, and to separate them from analog states  $(f_1 \leq 4)$ . The functions (35) and (36) are related by a unitary transformation analogous to the transformation from  $LS$  to  $jj$  coupling. In practical calculations, the preferable classification is the one in which the fragmentation of the state is minimal; of course, this also depends to a certain extent on the form of the  $\Lambda N$  interaction. Sometimes the choice of representation is dictated by the actual formulation of the problem. For example, decay of an excited state with emission of an  $s$ -shell hyperfragment  ${}^5_{\Lambda}\text{He}$ , which has the maximal spatial symmetry  $(f_1 = 5)$ , is allowed only if the wave function contains a “genuinely” hypernuclear component,<sup>83</sup> i.e., to describe this cluster decay channel, it is more convenient to use the representation (36).

In any form of the shell model, only a restricted number of oscillator quanta are taken into account in the construction of the basis wave functions. Several  $\hbar\omega$  can be taken into account only for simple nuclear systems.<sup>84</sup> Most authors<sup>38,42,75</sup> construct basis functions solely from  $0\hbar\omega$  and  $1\hbar\omega$  configurations. In such a case, one ignores the redistribution of the nucleons among the shell states that can, in general, arise on the addition of the hyperon and leads to a change in the properties of the nuclear core compared with its properties in the free state.



A very popular method for studying the changes in the radial density of nucleons due to the presence of a hyperon is the resonating-group model,<sup>85</sup> which is, essentially, an improved form of the  $\alpha$ -cluster model.<sup>86</sup> Developed in detail in nuclear theory, the resonating-group model has been widely used in the systematic description of the structure of light hypernuclei<sup>53,87</sup> with  $A \leq 9$ , treated as three-body systems of the form  $\alpha + x + \Lambda$  ( $x = N, d, t, \alpha$ ). It is well known<sup>56</sup> that the TISM and resonating-group model have much in common—in both, the center-of-mass motion is eliminated, and wave functions completely antisymmetrized with respect to all nucleons are used. Moreover, the wave functions in the two approaches are identical if the states in the TISM are classified in the  $LS$  coupling scheme and the lowest oscillator states are ascribed to the relative-motion functions of the clusters in the resonating-group model. Obviously, many properties of hypernuclear states can be described equally well in the two models if the corresponding parameters of the models are suitably chosen.

It is also known that in hypernuclei there are certain states that can be described comparatively simply in one model but whose description presents great technical difficulties in the other. As illustration, we give two examples.

1. The first example concerns the description of bands of levels of many-particle nuclear systems corresponding to broken nucleon clusters. They include, for example, levels with a hole in the  $s$  shell. A clear advantage of the TISM is its ability to describe such a state, in particular, the excited levels with  $T=1$  in  ${}^6\text{Li}$  and  ${}^8\text{Be}$  and other nuclei. These excitations cannot be considered in the cluster decompositions  $\alpha + d$  or  $\alpha + \alpha$ ,<sup>53,54</sup> but, as is well known, they are realized in  $(K^-, \pi^-)$  reactions with replacement of a neutron by the  $\Lambda$  hyperon on the targets  ${}^6\text{Li}$ ,  ${}^9\text{Be}$ , etc. A more complete description of the  ${}^9\text{Be}$  spectrum requires consideration of  ${}^8\text{Be}$  with one broken  $\alpha$  particle as a three-body system and the  ${}^9\text{Be}$  hypernucleus as a four-body system.<sup>88</sup> In the TISM, the transition from the one decomposition to the other ( $\alpha + \alpha \rightarrow {}^7\text{Be} + n$ ) is realized simply by a Talmi-Moshinsky-Smirnov transformation, and the hypernuclear problem itself is practically no more complicated.

At the same time, the approach of the resonating-group model provides a possibility for considering the change in the relative motion of the clusters due to the addition of the hyperon to the nuclear medium. An interesting result of the cluster model<sup>53,54,87</sup> is that the addition of the hyperon to the nuclear system can significantly change the relative motion of the nucleon clusters and, therefore, the probabilities of electromagnetic transitions. It is a difficult problem to take into account such effects in the shell model, since to do so it is necessary to include configurations with a larger number of oscillator quanta.

2. The resonating-group model also predicts qualitatively new effects<sup>53,87</sup> in heavier hypernuclei, for which it is necessary to take into account different cluster decompositions. A clear example is provided by the hypernucleus  ${}^{20}_{\Lambda}\text{Ne}$ . It is well known<sup>89</sup> that the spectrum of the lowest negative-parity states in the  ${}^{19}\text{Ne}$  nuclear subsystem begins very low, at 280 keV. In the cluster model, the low-lying

positive-parity  ${}^{19}\text{Ne}$  levels are described by the decomposition  $\{{}^{16}\text{O} + {}^3\text{He}\}$ , and the negative-parity levels by the decomposition  ${}^{15}\text{O} + {}^4\text{He}$ . It was shown in Ref. 90 that addition of the hyperon lowers the negative-parity states in  ${}^{20}_{\Lambda}\text{Ne}$ , and the ground state of the hypernucleus is the state  $\Lambda({}^{15}\text{O} + {}^4\text{He}) \otimes s_{\Lambda}:1^-$ , whereas the lowest positive-parity state  $\Lambda({}^{16}\text{O} + {}^3\text{He}) \otimes s_{\Lambda}:0^+$  is 2 MeV higher. The standard shell model gives a different order of the levels in  ${}^{20}_{\Lambda}\text{Ne}$ —the first two levels are  $0^+$  (ground state) and  $1^+$  (0.25 MeV) [doublet formed on the  $(1^+ / 2)^{19}\text{Ne}$  ground state], and the  $1^-$  level appears at a higher level, at excitation energy 0.7 MeV (Ref. 38). To test the different predictions of the cluster and shell models, it is proposed to use measurement of the  ${}^{20}_{\Lambda}\text{N}$  excitation functions in  $(K^-, \pi^-)$  and  $(\pi^+, K^+)$  reactions<sup>88</sup> or to detect delayed nuclear  $\gamma$  rays in mesonless weak decays of  ${}^{20}_{\Lambda}\text{Ne}$  (Ref. 91).

Comparing many results of the resonating-group model and the TISM, one can draw the general conclusion that the two models complement each other quite well and, taken together, can not only describe all the existing experimental data but can also predict new effects.

The change in the properties of the nucleon core due to the presence of a hyperon can also be studied in the framework of the hyperspherical-function method,<sup>92</sup> in which a collective variable, the hyperradius, is used. This method is used above all to describe individual global properties of hypernuclei—the binding energies and sizes of the hypernuclei, and the compressibility of the nuclear core.<sup>93,94</sup>

The variational approaches and methods of exact solution of the Schrödinger equation are used in the theory of hypernuclei mainly to interpret the properties of  $s$ -shell hypernuclei, namely, the ground ( $0^+$ ) and excited ( $1^+$ ) states of  ${}^4_{\Lambda}\text{H}$  and  ${}^4_{\Lambda}\text{He}$  and the binding energy  $B_{\Lambda}$  of the hypernucleus  ${}^5_{\Lambda}\text{He}$ . A problem here is that if one uses two-particle  $\Lambda N$  potentials of simple form that are consistent with the available data on  $\Lambda p$  scattering and the binding energies  $B_{\Lambda}$  for the hypernuclei with  $A=3$  and 4, one obtains excitation energies of  ${}^4_{\Lambda}\text{H}$  ( ${}^4_{\Lambda}\text{He}$ ) that are too low and a value of  $B_{\Lambda}$  that is too large (more than 5 MeV) for  ${}^5_{\Lambda}\text{He}$  ( $B_{\Lambda}^{\text{exp}} = 3.12 \pm 0.02$  MeV; Ref. 44). It appears that a simultaneous description of these systems and of hyperon-nucleon scattering can be achieved by introducing a two-channel interaction with coupling of the  $\Lambda$  and  $\Sigma$  channels<sup>95</sup> (solution of Faddeev equations) or by including in the problem effective (dispersive) spin-dependent  $\Lambda NN$  forces, which arise in the equations describing hypernuclei as a result of elimination of the  $\Sigma$  channel (variational approach<sup>96</sup>). Attempts are also made in the framework of the variational method to give a simultaneous description of  $\Lambda p$  scattering and the properties of the hypernuclei with  $A=3-5$  by adopting a more complicated form of the two-particle  $\Lambda N$  potentials.<sup>97</sup> As is emphasized in theoretical studies, for further advance in the solution of problems relating to the physics of few-nucleon hypernuclei it is important to have more accurate information about the cross sections for hyperon-nucleon scattering and the  ${}^3_{\Lambda}\text{He}$  binding energy ( $B_{\Lambda}^{\text{exp}} = 0.13-0.05$  MeV).<sup>44</sup>

For the shell description of the states of hypernuclei of intermediate mass ( $2d$  and  $2s$  shells) and of heavier ones

excited in  $(K^-, \pi^-)$  reactions, the number of required configurations increases sharply. In actual calculations of the gross structure of the excitation spectra of such systems, a restriction is made to approximate methods that use the notion of an "inert" core and valence nucleons. Since many hypernuclear states have a high position in the continuous spectrum, it is necessary to have measurements of their spectra with high energy resolution and separation of the contributions of the resonance and quasielastic reaction mechanisms.

In a wide range of mass numbers, the Hartree-Fock method is one of the common approaches to the study, at the microscopic level, of many properties of hypernuclei—the hyperon binding energies  $B_\Lambda$ , the quadrupole deformations and sizes of the hypernuclei, the Coulomb energy, the compressibility of the nuclear core, and the single-particle energy of the  $\Lambda$  hyperon.<sup>99</sup> A special interest in ways to describe the single-particle motions in hypernuclei and, in particular, in the possibilities of the Hartree-Fock method, arose as a result of the mastering of  $(\pi, K^+)$  reactions in the spectroscopy of  $\Lambda$  hypernuclei,<sup>21</sup> in which for hypernuclei with  $A=9-89$  experimental data were obtained on the single-particle energies of the  $\Lambda$  hyperon, beginning with the deepest shells and ending with the  $g$  shell in the hypernucleus  ${}^{89}_\Lambda\text{Y}$ . These data were recently analyzed in two ways—using simple approximations (Woods-Saxon potential, etc.)<sup>32</sup> and by the Hartree-Fock method with  $\Lambda N$  and  $\Lambda NN$  forces of Skyrme type.<sup>81</sup> The observed  $A$  dependence of the energy splitting between the  $(1p, 0s)$  and  $(2d, 1p)$  shells indicates an appreciable contribution of  $\Lambda NN$  forces. The question of the conditions under which density-dependent  $\Lambda N$  forces and  $\Lambda NN$  forces are equivalent was considered in the Hartree-Fock approach<sup>100</sup> and in a two-body model.<sup>101</sup>

Attempts are being made<sup>102-105</sup> to extend to hypernuclei the new methods being developed in nuclear theory for relativistic description of the single-particle motion of baryons.<sup>106</sup> To test the relativistic effects, it is proposed to measure the magnetic moments of hypernuclei with closed nucleon shells,<sup>102</sup> and also the cross sections of  $(e, e'K^+)$  and  $(\gamma, K^+)$  reactions.<sup>103, 104, 107</sup>

In recent years, ideas have been advanced about the possible manifestations of quark degrees of freedom in hypernuclei.<sup>32, 62, 108</sup> In the first place, there is the possibility of deconfinement of the strange quark in the nuclear medium if the hypernucleus is regarded as a system of  $3A$  quarks with the Pauli principle operating at the quark level. For example, in the  ${}^5_\Lambda\text{He}$  hypernucleus (mentioned above in connection with the difficulties in the description of  $B_\Lambda$ ) the  $ud$  quarks of the nucleons completely fill the  $0s$  orbit, and as a consequence of the Pauli principle the  $ud$  quarks of the hyperon must be placed in a higher orbit, whereas the  $s$  quark may be in a lower orbit, i.e., in the quark picture the complete nonidentity (distinguishability) of the hyperon and nucleon is destroyed. Such quark effects could also be reflected in the extent to which isospin purity is lost in various hypernuclear states<sup>62</sup> and in the  $A$  dependence of the splittings of the single-particle  $\Lambda$ -hyperon levels measured in  $(\pi^+, K^+)$  reactions.<sup>32</sup> However,

the existing experimental data are still entirely consistent with treatment of the  $\Lambda$  hyperon in the nucleus as a particle not identical to the nucleon, and a correct quantitative treatment of the problem of quark degrees of freedom appears to require measurements of higher accuracy.

#### 4. LOW-LYING STATES, ELECTROMAGNETIC TRANSITIONS, AND THE $\Lambda N$ INTERACTION IN HYPERNUCLEI

During the long period of establishment of hypernuclear physics by means of nuclear photoemulsions and bubble chambers, there were discoveries of individual modes of weak decays of the ground states of light hypernuclei with emission of pions, nucleons, and the lightest nuclei, and these gave information about the quantum numbers of some hyperfragments:  ${}^3_\Lambda\text{H}(1^+/2)$ ,  ${}^4_\Lambda\text{H}({}^4_\Lambda\text{He})(0^+)$ ,  ${}^8_\Lambda\text{Li}(1^-)$ ,  ${}^{11}_\Lambda\text{B}(5^-/2)$ ,  ${}^{12}_\Lambda\text{B}(1^-)$ .<sup>44, 109</sup> However, from the experience of the development of the spectroscopy of ordinary nuclei it was already clear then that other decays, characteristic of excited levels, with emission of  $\gamma$  rays, hyperons, nucleons, and nuclear clusters must play a no less important part in the development of ideas about the structure of hypernuclei and hyperon-nucleon forces.

Since in this part of the review we are in the first place interested in low-lying (below-threshold) levels of hypernuclei, it is appropriate to start by giving the existing experimental information about these levels, whose energies are determined from the spectra of the emitted  $\gamma$  rays. We shall then briefly consider the relations that determine the probabilities of  $\gamma$  transitions, and we shall complete this section with a discussion of the forms of the residual  $\Lambda N$  interaction and the general picture of hypernuclear spectra relating to the lowest configuration  $(p^{-1}s_\Lambda)$ .

##### Experimental data on hypernuclear $\gamma$ rays

Although this study is devoted to hypernuclei of the  $1p$  shell, for completeness of the information about the experiments so far made in  $\gamma$  spectroscopy it is also worth noting the first (mentioned in the Introduction) experiments on the detection of  $\gamma$  rays from the lightest  $s$ -shell hypernuclei  ${}^4_\Lambda\text{H}$  and  ${}^4_\Lambda\text{He}$ . The felicitously chosen target nuclei  ${}^6\text{Li}$  made it possible in a series of experiments involving the capture of stopped  $K^-$  mesons<sup>40-42</sup> and  $(K^-\pi^-\gamma)$  reactions "in flight"<sup>37</sup> to detect  $\gamma$  rays from  ${}^4_\Lambda\text{H}$  and  ${}^4_\Lambda\text{He}$ . For the  ${}^6\text{Li}$  target, no other sources of  $\gamma$  rays were expected, since even the ground state of  ${}^6_\Lambda\text{Li}$  can decay through the  $p + {}^5_\Lambda\text{He}$  channel. The threshold energy of the  $n + {}^5_\Lambda\text{He}$  channel for  ${}^6_\Lambda\text{He}$ , produced in the  $(K^-, \pi^0)$  reaction with stopped  $K^-$  mesons, is very small,  $240 \pm 10$  keV, so that most of the  ${}^6_\Lambda\text{He}$  states lie in the continuous spectrum and decay through baryonic channels. Experimental separation of the high region of  ${}^7_\Lambda\text{Li}$  excitation and the identification of  ${}^4_\Lambda\text{H}$  and  ${}^4_\Lambda\text{He}$  from the mesonic decays  ${}^4_\Lambda\text{H} \rightarrow {}^4\text{He} + \pi^-$  ( $E_\pi = 53$  MeV) and  ${}^4_\Lambda\text{He} \rightarrow {}^4\text{He} + \pi^0$  ( $E_\pi = 57$  MeV) made it possible to identify reliably  $\gamma$  lines with energies 1.04 and 1.15 MeV belonging to the hypernuclei  ${}^4_\Lambda\text{H}$  and  ${}^4_\Lambda\text{He}$ . The formation of  ${}^4_\Lambda\text{H}$  and  ${}^4_\Lambda\text{He}$  in excited

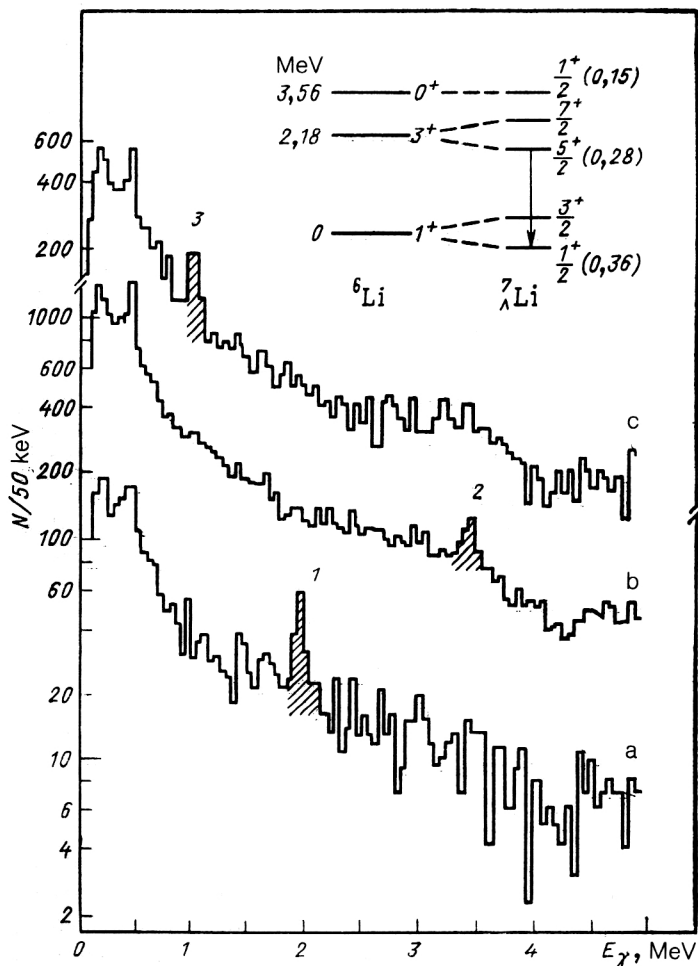


FIG. 1. Spectra of  $\gamma$  rays measured at BNL in the reaction  ${}^7\text{Li}(K^-, \pi^- \gamma){}_\Lambda^7\text{Li}$  at  $\theta_\pi \approx 0^\circ$  and  $P_K = 820 \text{ MeV}/c$  (Ref. 37) for three regions of  ${}^7\text{Li}$  excitation energy:  $-6$  to  $6 \text{ MeV}$  (a);  $6$ – $22 \text{ MeV}$  (b), and  $22$ – $39 \text{ MeV}$  (c); the hatched peaks are ascribed to  $\gamma$  transitions in  ${}_\Lambda^7\text{Li}[5^+/2 \rightarrow 1^+/2, E_\gamma = 2.034 \pm 0.023 \text{ MeV}]$  (1);  ${}^6\text{Li}(0^+ \rightarrow 1^+, E_\gamma = 3.56 \text{ MeV})$  (2);  ${}_\Lambda^4\text{He}(1^+ \rightarrow 0^+, E_\gamma \approx 1 \text{ MeV})$  (3). The spectra of  ${}^6\text{Li}$  and  ${}_\Lambda^7\text{Li}$  and the expected excitation intensities of the  ${}_\Lambda^7\text{Li}$  levels are shown at the top.<sup>74</sup>

$1^+$  states was interpreted as cluster decay of highly excited fragmented resonances with dominant configuration  $(s^{-1}s_\Lambda)$ .<sup>42,47</sup>

The slow accumulation of data on  $\gamma$  transitions in  $1p$ -shell hypernuclei is due in the first place to the unfavorable background conditions and low counting rate of events with excitation, in  $(K^-, \pi^-)$  reactions, of low-lying levels of the  $0\nu\omega$  configuration ( $p^{-1}s_\Lambda$ ) compared with excitation of levels of the  $1\nu\omega$  configuration ( $p^{-1}p_\Lambda$ ), especially those that are realized as a result of spin flip. The interest in  $\gamma$  spectroscopy of hypernuclei is high, since measurement of the energies of hypernuclear  $\gamma$  lines gives a very accurate position of the levels (to a few units or tens of kilo-electron-volts), which can be analyzed in various approaches. The existing experimental data, obtained mainly at BNL, are as yet few.

**${}_\Lambda^7\text{Li}$ .** In the  ${}^7\text{Li}(K^-, \pi^- \gamma){}_\Lambda^7\text{Li}$  reaction a  $\gamma$  line was observed<sup>37</sup> with energy  $E_\gamma = 2.034 \pm 0.023 \text{ MeV}$ , which is close to the energy of a  $\gamma$  transition in  ${}^6\text{Li}$ ,  $3^+, 0 \rightarrow 1^+, 0$  ( $E_\gamma = 2.19 \text{ MeV}$ ) and indicates detection of a hypernuclear  $\gamma$  transition [ $\frac{5}{2}^+ \rightarrow \frac{1}{2}^+$  (ground state)] between  ${}_\Lambda^7\text{Li}$  doublet states constructed on the levels  $3^+, 0$  and  $1^+, 0$  in  ${}^6\text{Li}$ . A previously reported<sup>110</sup>  $\gamma$  line with  $E_\gamma = 0.79 \text{ MeV}$  was not confirmed. A typical picture of the experimental  $\gamma$  spectra is shown in Fig. 1. The hypernuclear  $\gamma$  line with

$E_\gamma = 442.1 \pm 2.1 \text{ keV}$  detected in the  ${}^{10}\text{B}(K^-, \pi^- \gamma){}_\Lambda^{10}\text{B}$  reaction at high excitation energies of  ${}_\Lambda^{10}\text{B}$  ( $21$ – $29 \text{ MeV}$ )<sup>111</sup> was ascribed in Ref. 112 to the  $\gamma$  transition  $\frac{3}{2}^+ \rightarrow \frac{1}{2}^+$  (ground state) in the daughter hypernucleus  ${}_\Lambda^7\text{Li}$ . The hypernucleus  ${}_\Lambda^7\text{Li}$  is produced by cluster decay of a particle-hole substitution ( $s^{-1}s_\Lambda$ ) resonance in  ${}_\Lambda^{10}\text{B}$  through the channel  ${}^3\text{He} + {}_\Lambda^7\text{Li}^*$ . As was shown in Ref. 112, the decay of such a  ${}_\Lambda^{10}\text{B}$  state through the  $2p + {}_\Lambda^8\text{Li}$  channel proposed in Ref. 111 is strongly suppressed. In addition, the observed  $\gamma$  line does not correspond to the expected scheme of  ${}_\Lambda^8\text{Li}$  levels.

**${}_\Lambda^8\text{Li}$ .** Data on  $\gamma$  lines from  ${}_\Lambda^8\text{Li}$  are contradictory. In capture of stopped  $K^-$  mesons by the  ${}^9\text{Be}$  nucleus,  $\gamma$  rays were noted with  $E_\gamma = 0.31 \pm 0.02 \text{ MeV}$  (Ref. 39) and  $E_\gamma = 1.22 \pm 0.04 \text{ MeV}$  (Ref. 113), and they were ascribed to the daughter hypernucleus  ${}_\Lambda^8\text{Li}$  produced by decay of the excited hypernucleus  ${}_\Lambda^9\text{Be}$ . However, the authenticity of these  $\gamma$  lines (especially the second) has been questioned.<sup>114</sup>

**${}_\Lambda^9\text{Be}$ .** In the  ${}^9\text{Be}(K^-, \pi^- \gamma){}_\Lambda^9\text{Be}$  reaction a  $\gamma$  line was observed with  $E_\gamma = 3.079 \pm 0.04 \text{ MeV}$  (Ref. 37), which is close to the energy of the nuclear level  $2^+, 0$  ( $2.94 \text{ MeV}$ ) in  ${}^8\text{Be}$  and indicates observation of the  $\gamma$  transitions ( $\frac{3}{2}^+, \frac{5}{2}^+$ )  $\rightarrow \frac{1}{2}^+$  with nearly the same energy in  ${}_\Lambda^9\text{Be}$  following

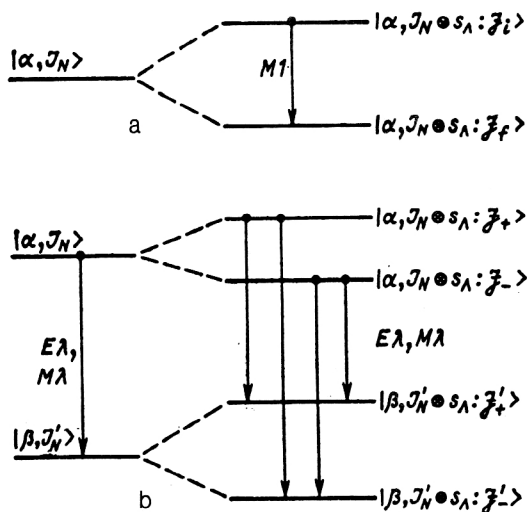


FIG. 2. Schematic representation of doublet splittings and  $\gamma$  transitions in hypernuclei: a)  $\gamma$  deexcitation of a level of an individual doublet; b) electromagnetic transitions between the levels of two different doublets.

deexcitation of the doublet formed on this nuclear level.

$^{10}_{\Lambda}\text{B}$ ,  $^{16}_{\Lambda}\text{O}$ . Searches for  $\gamma$  rays from the ground-state doublet of  $^{10}_{\Lambda}\text{B}$  were recently made in the  $^{10}\text{B}(K^-, \pi^- \gamma)^{10}_{\Lambda}\text{B}$  reaction.<sup>5,111</sup> Shell calculations with a standard form of the  $\Lambda N$  interaction<sup>38</sup> predicted for the  $\gamma$  transition  $2^-_1 \rightarrow 1^-$  (ground state) a  $\gamma$  line with  $E_\gamma \approx 160$  keV, but no such line was observed. The experiments showed (Refs. 111, 115, and 116) that the energy  $\Delta E(2^-_1, 1^-)$  of the doublet splitting in  $^{10}_{\Lambda}\text{B}$  must be less than 80–100 keV. The previously reported<sup>117</sup>  $\gamma$  line with  $E_\gamma \approx 160$  keV was not confirmed. The doublet splitting with  $\Delta E(1^-_1, 0^-) \approx 80$  keV of the  $^{16}_{\Lambda}\text{O}$  ground state predicted in Ref. 38 was not found in the  $^{16}\text{O}(K^-, \pi^- \gamma)^{16}_{\Lambda}\text{O}$  reaction.<sup>5,115,116</sup>

Data on  $\gamma$  transitions are of great interest in hypernuclear spectroscopy, since accurate measurements of the energies of hypernuclear levels are important for determining the parameters of the  $\Lambda N$  interaction. As will be seen from the following exposition, these data on  $\gamma$  lines do not exhaust the gamut of expected hypernuclear  $\gamma$  spectra.

### Probabilities of hypernuclear $\gamma$ transitions

Following Ref. 74, we briefly consider some general properties of  $\gamma$  transitions between hypernuclear states with a hyperon in the 0s shell. It is convenient to divide them into two groups—the  $\gamma$  deexcitation of the upper component of a doublet formed on a single nuclear state  $|\alpha J_N\rangle$  (Fig. 2a) and  $\gamma$  transitions between levels constructed on two different states  $|\beta J'_N\rangle$  and  $|\alpha J_N\rangle$  of the nuclear core, this corresponding qualitatively to weak binding of the  $\Lambda$  hyperon to the nucleus (Fig. 2b).

In the first case, the  $M1$  transition is dominant if the splitting of the doublet states is not too large, and the corresponding radiative width is determined by the expression

$$\Gamma_\gamma(M1) = \alpha_1 (\Delta E)^3 \frac{3}{2} (2J_f + 1) \times \begin{Bmatrix} J_i & J_f & 1 \\ 1/2 & 1/2 & J_N \end{Bmatrix}^2 (g_N - g_\Lambda)^2, \quad (37)$$

where  $\alpha_1 = 4.2 \times 10^{12} \text{ sec}^{-1} \cdot \text{MeV}^{-3}$ ;  $g_N$  and  $g_\Lambda$  are the nuclear and  $\Lambda$ -hyperon  $g$  factors that determine the magnetic moment  $\mu = gJ$ . The expression (37) is often used to estimate the lifetime  $\tau = \hbar/\Gamma_\gamma$  of the upper level of the doublet. If it is found to be shorter than the lifetime of the  $\Lambda$  hyperon in the nucleus [for the free hyperon,  $\tau_\Lambda \approx 2.63 \times 10^{-10} \text{ sec}$  (Ref. 118)], then weak (mesonic or mesonless) decay of the state will be dominant. Such states are called *isomer* states, and they are possible in hypernuclei of the  $1p$  shell.

Radiative transitions in the second group can be of the electric ( $E\lambda$ ) or magnetic ( $M\lambda$ ) types ( $\lambda$  is the multipolarity of the transition). The hypernuclear radiative width  $\Gamma_\gamma(\lambda)$  can be expressed simply in terms of the nuclear width  $\Gamma_N(\lambda)$ :

$$\Gamma_\gamma(\lambda) = (2J_N + 1)(2J_f + 1) \times \begin{Bmatrix} J'_N & J_f & \frac{1}{2} \\ J_i & J_N & \lambda \end{Bmatrix}^2 (E_{if}/E_N)^{2\lambda+1} \Gamma_N(\lambda). \quad (38)$$

The relation (38) is of interest for identifying the strongest expected hypernuclear  $\gamma$  transitions. Among the excited doublets there may also be isomer states, for example, in  $^7_\Lambda\text{He}$  such a level may be the  $5^+/2$  level constructed on the nuclear state  $2^+$ , 1 in  $^6\text{He}$ . There are, in fact, experimental indications of the existence of an isomer level in this hypernucleus.<sup>119</sup> Measurement of the probabilities of  $\gamma$  transitions of the second group make it possible, using (38), to determine the nuclear radiative width  $\Gamma_N(\lambda)$  in the presence of the  $\Lambda$  hyperon. Such data on the electromagnetic properties of the nuclear core have considerable interest for the theory of hypernuclear structure, since in individual cases, as calculations in the cluster model show, the radiative width  $\Gamma_N(\lambda)$  can differ strongly from the corresponding width  $\Gamma_N(\lambda)$  for the free nucleus.<sup>53–55</sup> Calculations of hypernuclear radiative widths have also been made in the shell model.<sup>74,120</sup> The expected values of  $\Gamma_\gamma$  for  $^4_\Lambda\text{H}$  ( $^4_\Lambda\text{He}$ ) can be found in Ref. 121. As yet there is no experimental information on hypernuclear radiative widths.

### Hypernuclear $\gamma$ transitions and parameters of the residual $\Lambda N$ interaction

During the last one and a half to two decades, as experimental data have accumulated on the  $\Lambda$ -hyperon binding energies  $B_\Lambda$  and excited levels of  $1p$ -shell hypernuclei, several forms of two- and three-particle potential parameters of the shell model have been proposed.<sup>70–72,122</sup> The first versions, based on reproducing  $B_\Lambda$ , included, besides the five independent parameters  $V$ ,  $\Delta$ ,  $S_\Lambda$ ,  $S_N$ , and  $T$  corresponding to the two-body interaction (31), additional parameters:  $Q^*$  (Ref. 71), or, later,  $Q^0_{00}$  (Ref. 72), the matrix



elements of two-pion three-particle  $\Lambda NN$  forces. With optimal form ( $\Delta + S + Q_{00}^0$ ;  $\chi^2 = 79$ ) of the parameters (in mega-electron-volts)

$$\begin{aligned}\bar{V} &= 1.23, \Delta = 0.15, S_\Lambda = 0.57, \\ S_N &= -0.21, T = 0, Q_{00}^0 = -0.14.\end{aligned}\quad (39)$$

The spectra and  $\gamma$ -transition probabilities in  $1p$ -shell hypernuclei from  ${}^7_\Lambda\text{He}$  to  ${}^{16}_\Lambda\text{O}$  were predicted in Ref. 74. However, subsequent experiments at BNL,<sup>37</sup> in which  $\gamma$  lines from  ${}^7_\Lambda\text{Li}$  and  ${}^9_\Lambda\text{Be}$  were detected, did not confirm the predictions of the theory for the positions of the levels  $5^+/2$  in  ${}^7_\Lambda\text{Li}$  and  $(3^+/2, 5^+/2)$  in  ${}^9_\Lambda\text{Be}$ . There was also no confirmation of the results of the shell calculation<sup>122</sup> of the spectra of  ${}^7_\Lambda\text{Li}$  and  ${}^9_\Lambda\text{Be}$ , in which the five matrix elements  $\langle p_{j_1} s_\Lambda : J | V | p_{j_2} s_\Lambda : J \rangle$ , found by the least-squares method from  $B_\Lambda$ ,<sup>3)</sup> were used as parameters.

Even before the experiment of Ref. 37, very cautious conclusions were drawn in Refs. 70–72 concerning the reliability of the recovery of parameters of the shell model from (experimental)  $B_\Lambda$ . What is unsatisfactory is the existence of several solutions that minimize the quadratic deviations of the theoretical  $B_\Lambda$  from the experimental  $B_\Lambda$ . Besides the  $\chi^2$  test, selection was made using additional conditions such as reproduction of the known total angular momenta of  ${}^8_\Lambda\text{Li}(1^-)$ ,  ${}^{11}_\Lambda\text{B}(5^+/2)$ ,  ${}^{12}_\Lambda\text{B}(1^-)$  (Ref. 44), the requirement of a not too large value of  $\Delta = \Delta_s - \Delta_n$ , which specifies the difference of the singlet and triplet interactions motivated by analysis of  $\Lambda p$  scattering cross sections, etc. In addition, the unsatisfactory situation with regard to the determination of the parameters of the model from  $B_\Lambda$  suggests that it is insufficient in calculations of  $B_\Lambda$  to use the simple shell configuration  $\{s^4 p^n \otimes s_\Lambda : \mathcal{J} T\}$ . The need for inclusion in such calculations of more complicated configurations appears necessary if it is recalled that  $B_\Lambda$  is the difference of the total energies of the nucleus and hypernucleus. However, it is not easy to make such calculations because of the large number of matrix elements.

To overcome the difficulties that arise with the interpretation of the hypernuclear spectra, a different method was used in Ref. 38 to determine  $\Delta$ ,  $S_\Lambda$ ,  $S_N$ , and  $T$  without explicit introduction of three-particle parameters. The parameter  $\Delta$  was estimated with a Gaussian shape of the  $\Lambda N$  potential  $V_\sigma(r)$  from the known energy ( $\approx 1$  MeV) of the  $M1$   $\gamma$  transition  $1^+ \rightarrow 0^+$  in  ${}^4_\Lambda\text{H}$  ( ${}^4_\Lambda\text{He}$ ) (Refs. 39 and 41). The value of  $S_\Lambda$  was determined from the spin-orbit splitting of the single-particle state of the  $\Lambda$  hyperon in the  $1p$  shell,  $\varepsilon_p(\Lambda) = \varepsilon_{p_{1/2}}(\Lambda) - \varepsilon_{p_{3/2}}(\Lambda) = 0.36 \pm 0.3$  MeV, found from the difference between the energies of the  $1^-/2$  and  $3^-/2$  levels in  ${}^{13}_\Lambda\text{C}$  (Ref. 123) and the experimental bound<sup>37</sup> on the doublet splitting of the levels in  ${}^9_\Lambda\text{Be}$ :  $\Delta E(3^+/2, 5^+/2) \lesssim 100$  keV. The other two parameters,  $S_N$  and  $T$ , were chosen on the basis of the properties of the free hyperon-nucleon interaction.<sup>79</sup> The result was the proposal of a new (standard) set of parameters,

$$\Delta = 0.5; S_\Lambda = -0.04; S_N = -0.08; T = 0.04, \quad (40)$$

which gives a reasonably good description of the energy of the  $\gamma$  transition  $5^+/2 \rightarrow 1^+/2$  in  ${}^7_\Lambda\text{Li}$  with  $E_\gamma = 2.034 \pm 0.023$  MeV [ $E_\gamma(\text{theor}) = 2.24$  MeV], the mixing parameter in the wave function of  ${}^8_\Lambda\text{Li}(\mathcal{J}^\pi = 1^-)$  (Ref. 124), and the possible  $\gamma$  line with  $E_\gamma = 0.31 \pm 0.02$  MeV [ $E_\gamma(\text{theor}) = 0.33$  MeV] in  ${}^8_\Lambda\text{Li}$ .<sup>38,39</sup> Note that these calculations were made with Cohen–Kurath nuclear wave functions with parameters of the  $NN$  interaction taken to be the same for  $1p$ -shell nuclei with  $A = 6$ –14 (Ref. 125). In Ref. 38 the need for experimental verification of the predicted doublet splittings in the hypernuclei, which depend mainly on just three parameters,  $\Delta$ ,  $S_\Lambda$ , and  $T$ , was especially emphasized. The position of the doublet centroids depends on the parameter  $S_N$ . The three-particle  $\Lambda NN$  forces can influence the effective value of  $S_N$ . As we have already noted, the recent BNL experiments<sup>111,115,116</sup> did not find the  $\gamma$  lines expected on the basis of the calculations of Ref. 38 from the ground-state doublets of  ${}^{10}_\Lambda\text{B}$  and  ${}^{16}_\Lambda\text{O}$ , indicating that some of the parameters in the set (40) are not realistic.

A search for new shell-model parameters permitting the description of the known experimental data on  $\gamma$  transitions in  ${}^7_\Lambda\text{Li}$  and  ${}^9_\Lambda\text{Be}$  together with the small doublet splittings in  ${}^{10}_\Lambda\text{B}$  and  ${}^{16}_\Lambda\text{O}$  was made in Ref. 126. In contrast to the earlier investigations (Refs. 38, 71, 72, and 122), the parameters  $\Delta$ ,  $S_\Lambda$ ,  $S_N$ , and  $T$  were not related to the values of  $B_\Lambda$  or to the splitting of the  $0^+$  and  $1^+$  levels in  ${}^4_\Lambda\text{H}$  ( ${}^4_\Lambda\text{He}$ ) (the method of estimating  $\Delta$  in Ref. 38) but were taken purely phenomenologically and found from experimental data on certain hypernuclear levels, namely: (a)  $E(2^-_1) - E[1^- (\text{ground state})] = E(2^-_1, 1^-) \leq 100$  keV for  ${}^{10}_\Lambda\text{B}$  and  $\Delta E(1^-_1, 0^-) (\text{ground state}) \leq 100$  keV for  ${}^{16}_\Lambda\text{O}$ ; (b)  $\Delta E(3^+/2, 5^+/2) \leq 100$  keV for  ${}^9_\Lambda\text{Be}$ ; (c)  $E(5^+/2) = 2.034 \pm 0.023$  MeV for  ${}^7_\Lambda\text{Li}$ , the aim being to ensure the total angular momentum and parity  $\mathcal{J}^\pi = 1^-$  for  ${}^{12}_\Lambda\text{B}$  known from analysis of weak decays. It was found that the spins of the  ${}^{11}_\Lambda\text{B}$  and  ${}^8_\Lambda\text{Li}$  ground states can also be reproduced. This way of determining the parameters and describing the spectra of the hypernuclei (nuclei) of the  $1p$  shell in the framework of the simple configuration  $\{s^4 p^n \otimes s_\Lambda\}(\{s^4 p^n\})$  appears to be more reliable than calculation of the single-particle energies ( $B_\Lambda$ ) of the  $\Lambda$  hyperon, which, like the nucleon binding energies, can depend on many factors, for example, the admixtures of more complicated configurations, details of the cluster structure of the hypernucleus, etc. The expediency of choosing the parameters of the  $\Lambda N$  forces on the basis of the spectra of hypernuclei was pointed out earlier in the studies of Ref. 73, which investigated the dependence of the level energies on the parameter  $\Delta$ .

As a result of the analysis of Ref. 126, which was made with the nuclear wave functions of Barker ( $6 \leq A \leq 9$ )<sup>127</sup> and Cohen and Kurath ( $10 \leq A \leq 14$ ), the following optimal set of parameters was obtained by means of relations of the form (33):<sup>4)</sup>

$$\begin{aligned}\Delta &= 0.3; S_\Lambda = -0.02; T = 0.02; \\ S_N &= -0.35 \text{ for } {}^7_\Lambda\text{Li} \text{ (variant SL);}\end{aligned}\quad (41)$$

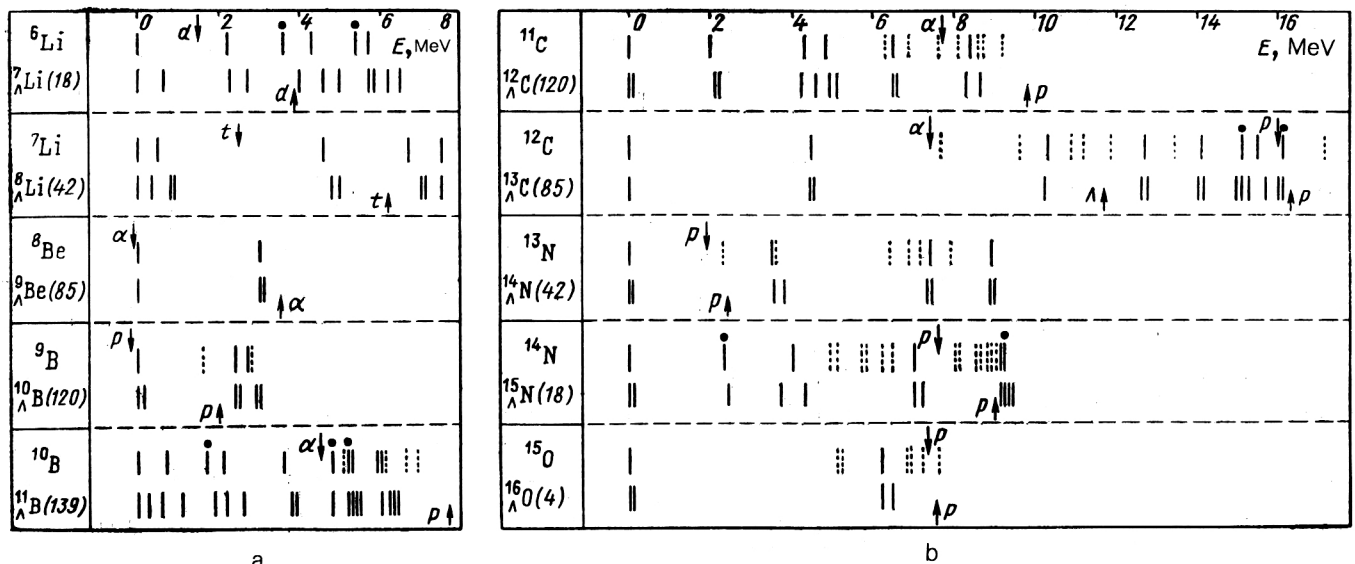


FIG. 3. Levels of nuclei and hypernuclei of the  $1p$  shell and stability threshold for  ${}^6\text{Li}$ ,  ${}^7\text{Li}$ – ${}^{10}\text{B}$ ,  ${}^{11}\text{B}$  (a) and  ${}^{11}\text{C}$ ,  ${}^{12}\text{C}$ – ${}^{15}\text{O}$ ,  ${}^{16}\text{O}$  (b).

$S_N = -0.1$  for  $7 < A \leq 16$  (variant SG).

The increase of  $|S_N|$  compared with  $S_{N\text{stand}}$  in (40) was attributed in Ref. 126 to the influence of the cluster structure of  ${}^7\text{Li}$ . The conclusion of a need to reduce the value of  $\Delta$  compared with  $\Delta_{\text{stand}}$  is strengthened by the result of Ref. 128, in which it was emphasized that only part (2/3) of the doublet splitting  $\Delta E_{\text{exp}}(1^+, 0^+) \simeq 1$  MeV in  ${}^4\text{H}$  ( ${}^4\text{He}$ ) could be explained by the contribution of the two-particle  $\Lambda N$  interaction  $V_o(r)S_N S_\Lambda$ , the missing fraction of the splitting being due to the influence of the  $\Sigma$  channel, which can be taken into account by introducing dispersive three-particle  $\Lambda NN$  forces with a dependence on the spin of the  $\Lambda$  hyperon. The insufficiency of introducing just a spin-dependent  $\Lambda N$  interaction in order to explain the position of the  $1^+$  level in hypernuclei with  $A=4$  was also pointed out in Ref. 95, in which the many-particle aspects of the description of these hypernuclei were taken into account.

Further experimental verification of the hypernuclear spectra predicted by the shell model with the new set of parameters (41) would be of great interest.

## 5. GENERAL FEATURES OF HYPERNUCLEAR SPECTRA AND THEIR EXCITATION IN REACTIONS WITH AND WITHOUT SPIN FLIP

In  $1p$ -shell hypernuclei there are in general expected to be many (several hundred) states with  $(p^{-1}s_\Lambda)$  configuration, which can be described by the wave functions (26). Among them there are several tens of below-threshold (bound) levels, which must decay with the emission of  $\gamma$  rays.

If one does not attempt a high-precision description of the positions of the levels (allowing an error of order 100–200 keV), the general features of the hypernuclear spectra and the intensities of their excitation are not especially sensitive to changes in the potential parameters discussed

above [the sets (40) or (41)]. Bearing this in mind, we give here only preliminary recommendations for new experiments in the  $\gamma$  spectroscopy of hypernuclei. A more detailed discussion of the systematics of the spectra is deferred to Sec. 6.

Figures 3a and 3b shows bands of spectra of hypernuclei from  ${}^7\text{Li}$  to  ${}^{16}\text{O}$  calculated with the parameters (40) by diagonalizing the energy matrices up to excitation energies of about 17 MeV. Next to the symbols of the hypernuclei, we give in brackets the total numbers of hypernuclear states with the configuration  $\{s^4 p^n \otimes s_\Lambda; JT\}$ . Opposite the symbols of the core nuclei ( ${}^6\text{Li}$ ,  ${}^7\text{Li}$ , etc.) we give the nuclear spectra corresponding to the configuration  $\{s^4 p^n; JT\}$ . Levels of the hypernuclei (nuclei) with values of the isospin greater than for the ground state ( $T=3/2$  or  $T=1$ ) are indicated by heavy black dots. The calculations were made with the Cohen–Kurath nuclear wave functions.<sup>125</sup> When possible, the values of the nuclear energies were taken from experiment.<sup>82</sup> For completeness of the picture, the nuclear spectra are augmented with states (dotted lines) described by other, more complicated configurations (intruder states). The hypernuclear levels formed on them do not play a significant role in the single-particle hypernuclear production reactions.<sup>74</sup> The arrows show the threshold energies for emission of a proton, deuteron,  $\alpha$  particle, and  $\Lambda$  hyperon. It can be seen from comparison of the nuclear and hypernuclear spectra with the stability thresholds that the addition to a nucleus of a  $\Lambda$  hyperon in the  $0s$  state raises the stability of the system. Because of the higher thresholds in the  $1p$ -shell hypernuclei, there are more bound states than in the corresponding nuclei. Some of them may be isomer states, but the majority of the excited levels must decay with the emission of  $\gamma$  rays. In individual cases, there can be  $\gamma$  deexcitation of hypernuclear states in the continuous spectrum if the strong decay channel is forbidden by the isospin selection

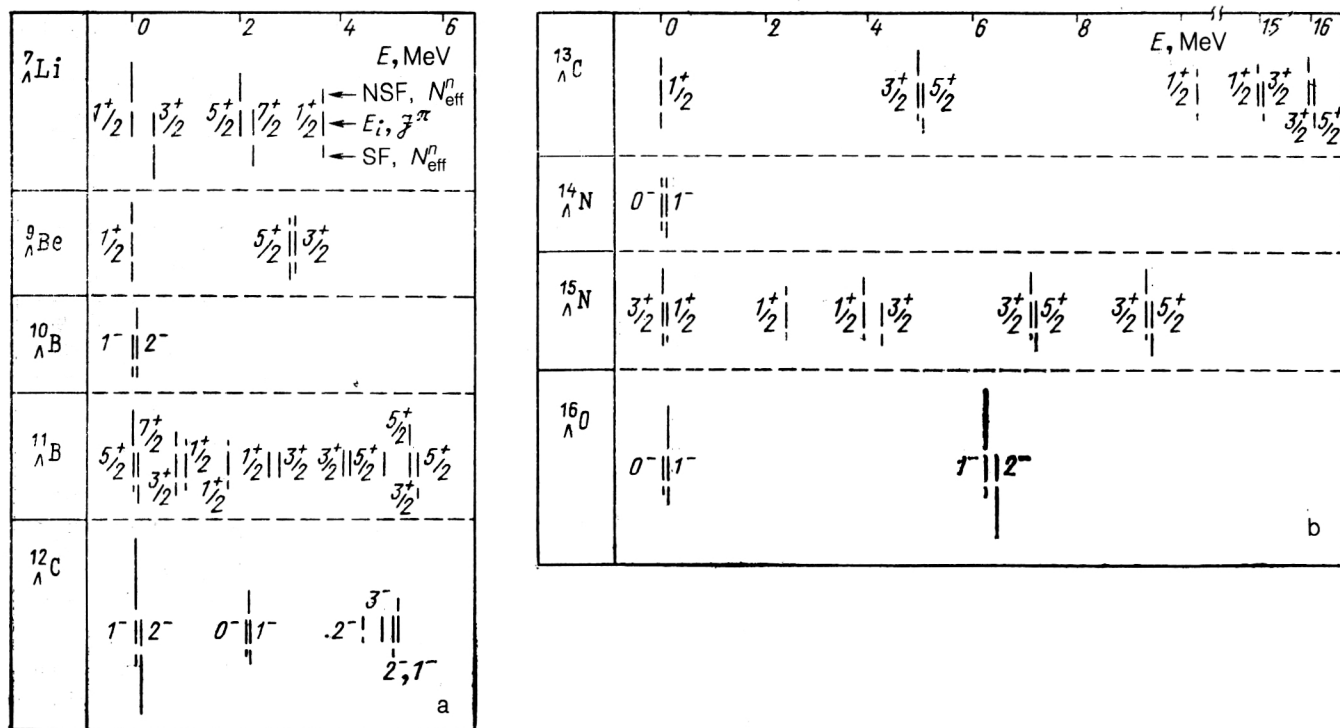


FIG. 4. Hypernuclear levels below the stability thresholds and effective numbers of neutrons ( $N_{\text{eff}}^n$ ) in reactions with spin flip (SF) and without spin flip (NSF) for  ${}^7_{\Lambda}\text{Li}$ - ${}^{12}_{\Lambda}\text{C}$  (a) and  ${}^{13}_{\Lambda}\text{C}$ - ${}^{16}_{\Lambda}\text{O}$  (b). Also shown are the  ${}^{13}_{\Lambda}\text{C}$  states in the continuous spectrum at 15–16 MeV, the  $\Lambda$ - and  $\alpha$ -decay of which is forbidden by the isospin selection rule.

rule [an example is provided by the  $^{13}\text{C}$  levels at  $E=15\text{--}16$  MeV (Refs. 43 and 83)]. Identification and measurement of the energies of hypernuclear  $\gamma$  lines is one of the direct ways of testing models of hypernuclei.

The nuclear reactions ( $K^-, \pi^-$ ) (Ref. 2) and ( $K^-, \pi^- \gamma$ ) (Refs. 37, 111, 115, and 116) and the recently mastered<sup>21</sup> processes ( $\pi^+, K^+$ ) are successfully used in hypernuclear spectroscopy in a wide range of mass numbers. It has been established that they are realized by a single-particle mechanism, in which one of the  $1p$  neutrons is transformed for the configurations of the nuclei and hypernuclei considered here into a  $\Lambda$  hyperon in the  $0s$  shell as a result of  $K^- n \rightarrow \pi^- \Lambda$  or  $\pi^+ n \rightarrow K^+ \Lambda$  reactions. At the same time, there is an angular-momentum transfer  $\Delta L = 1$ , and the nucleus  $\rightarrow$  hypernucleus transition can take place both with and without spin flip. These two types of reactions (spin-flip processes of hypernuclear formation have not yet been studied) must, as a rule, lead to different excitation intensities of the individual components of hypernuclear doublets.

In order to give some preliminary recommendations concerning further experiments to look for new hypernuclear  $\gamma$  rays, we give in Figs. 4a and 4b, in addition to the spectra and quantum numbers of the bound hypernuclear levels, the intensities, in relative units, of their excitation, or, rather, the effective numbers of neutrons ( $N_{\text{eff}}^n$ ) for reactions without spin flip (vertical lines above the spectrum) and with spin flip (lines below the spectrum). The results of the calculations presented in Figs. 4a and 4b were obtained with a set of parameters (SG) made consistent,

by the method described in the previous section, with the available data on the levels of  $1p$ -shell hypernuclei. It is well known that in  $(K^-, \pi^-)$  reactions at kaon momenta less than  $1 \text{ GeV}/c$  transitions without spin flip are dominant in a wide interval of pion emission angles.<sup>2</sup> Transitions with spin flip make a significant contribution to the  $(\pi^+, K^+)$  reaction for  $K^+$  emission angles  $\theta_k \geq 10\text{--}15^\circ$ .<sup>50</sup> Suitable reactions for investigating spin-flip excitations could be the  $(\gamma, K^0)$  or  $(e, e'K^+)$  processes,<sup>107,129</sup> which are realized on protons of a target nucleus but have not yet been studied experimentally. It can be seen from Figs. 4a and 4b (very small values of  $N_{\text{eff}}^n$  are not shown) that the individual components of the doublets are excited differently, depending on the type of transition. Of course, there are also other ways of populating hypernuclear states, for example, in secondary processes—in nucleon or cluster decays of the original hypernuclear resonance.<sup>43,130</sup> The excitation functions of the hypernuclear states shown in Figs. 4a and 4b depend weakly on the doublet splittings, i.e., on the values of the shell-model potential parameters  $\Delta$ ,  $S_\Lambda$ ,  $S_N$ , and  $T$  considered in the investigation.

Using Figs. 4a and 4b, one can make a number of comments concerning the possibilities of  $\gamma$  spectroscopy of hypernuclei in the  $(K^-, \pi^- \gamma)$  and  $(\pi^+, K^+ \gamma)$  reactions. In Refs. 111, 115, and 116, it was not possible to detect  $\gamma$  lines from the ground-state doublets  $(2_1^-, 1^-)$  in  $^{10}_\Lambda\text{B}$  and  $(1_1^-, 0^-)$  in  $^{16}_\Lambda\text{O}$  because of the smallness of the corresponding splittings:  $\Delta E \leq 80\text{--}100$  keV. It is entirely possible that the upper components of the doublets in these hyper-

TABLE I. Spectrum of levels of the hypernuclei  ${}^7_{\Lambda}\text{Li}$ ,  ${}^8_{\Lambda}\text{Li}$ ,  ${}^9_{\Lambda}\text{Be}$ , and  ${}^{10}_{\Lambda}\text{Be}$ , lowest disintegration thresholds, and effective neutron numbers ( $N_{\text{eff}}^n$ ). For  ${}^{10}_{\Lambda}\text{B}$ , the result obtained with the set SG(10, 16) is shown in the brackets.

$^A_Z\Lambda$	$E_{\text{stab}}, \text{MeV}$	$E_N, \text{MeV}$	$J_N T_N$	$N_{\text{eff}}^n \%$		$J$	SG	SL	ST	KSA [120]	WBT [87]		
				NSF	SF						S, YNG	L, YNG	L, ORG
											$E, \text{MeV}$		
$^7_{\Lambda}\text{Li}$	3,93 (d)	0	1 0	39 1	5 35	1/2 3/2	0 0,44	0 0,44	0 0,61	0 0,79	0 1,33	0 1,33	0 1,1
		2,19	3 0	30	7 23	5/2 7/2	2,03 2,30	2,07 2,29	2,24 2,68	2,38 3,01	1,83 3,1	2,14 3,34	1,99 2,92
		3,56	0 1	14	14	1/2	3,64	3,64	3,96	4,09	—	—	—
$^8_{\Lambda}\text{Li}$	6,15 (t)	0	3/2 1/2			1 2	0 0,3	0 0,24	0 0,33	0 0,46	— —	0 0,83	0 0,66
		0,48	1/2 1/2			0 1	0,8 0,82	0,84 0,94	0,81 0,86	{ 1,13 0,65	— —	1,43 1,29	1,36 1,22
$^9_{\Lambda}\text{Be}$	3,50 ( $\alpha$ )	0	0 0	18	18	1/2	0	0	0	0	—	0	0
		2,94	2 0	9 16	17 8	5/2 3/2	3,05 3,11	3,03 3,10	2,90 3,01	{ 2,95 2,93	— —	3,12	3,06
$^{10}_{\Lambda}\text{B}$	2,00 (p)	0	3/2 1/2	18	9 9	1 2	0 0,1 (0,08)	0 0,06	0 0,17	0 0,24	0 0,16 IMB [131]	— —	— —

nuclei are isomer states and that their  $\gamma$  deexcitation is strongly suppressed. Although  $\gamma$  rays from the excited  $(3^+/2, 5^+/2)$  doublet in  ${}^9_{\Lambda}\text{Be}$  have been detected,<sup>37</sup> for this hypernucleus one can pose the problem of resolving the close  $\gamma$  lines in the  $(3^+/2, 5^+/2) \rightarrow 1^+/2$  transitions. In the hypernuclei  ${}^{12}_{\Lambda}\text{C}$  and  ${}^{14}_{\Lambda}\text{N}$ , the doublet splittings are small,  $\Delta E(2_1^-, 1^-) \approx 80$  keV and  $\Delta E(1^-, 0^-) \approx 10$  keV, and therefore the corresponding levels are expected to be isomers. The search for  $\gamma$  lines from the excited  $(0^-, 1_2^-)$  doublet ( $E \approx 2$  MeV) in  ${}^{12}_{\Lambda}\text{C}$  is complicated by the fact that a large fraction of the  ${}^{12}_{\Lambda}\text{C}$  excitation intensity is concentrated on the ground-state doublet  $(2_1^-, 1^-)$ . The values of  $N_{\text{eff}}^n$  shown in Figs. 4a and 4b were calculated in the weak-binding limit. In the case of  ${}^{12}_{\Lambda}\text{C}$  inclusion of the  $\Lambda N$  interaction merely enhances the dominance of the excitation of the  $(2_1^-, 1^-)$  doublet. In  ${}^{11}_{\Lambda}\text{B}$  and  ${}^{15}_{\Lambda}\text{N}$ , the number of bound levels is quite high (around ten), but because their occupation is strongly fragmented unambiguous identification of the  $\gamma$  lines may be a complicated problem. Also of practical interest are searches for new  $\gamma$  transitions in  ${}^7_{\Lambda}\text{Li}$  from deexcitation of the upper level of the ground-state  $3^+/2$  doublet and higher levels and for  $\gamma$  transitions from the excited doublets with energies around 4.5 MeV and 15–16 MeV in  ${}^{13}_{\Lambda}\text{C}$  and 6.2–6.4 MeV in  ${}^{16}_{\Lambda}\text{O}$ .

## 6. SPECTROSCOPY OF 1p-SHELL HYPERNUCLEI

Having at our disposal the new approximate set of potential parameters (41), we return, but now at a more

detailed level, to the problem considered in Sec. 4, namely, that of low-lying hypernuclear spectra, the intensities of their excitation in different reactions (with and without spin flip), and  $\gamma$  transitions in hypernuclei. In the process, we shall give the dependences of the energies of the individual hypernuclear levels on the parameters that, from our point of view, are the most interesting for  $\gamma$  spectroscopy of 1p-shell hypernuclei.

### Energy spectra of hypernuclei, excitation intensities of levels, and $\gamma$ transitions

The energies of levels of 1p-shell hypernuclei ( ${}^A_Z\Lambda$ ,  $7 \leq A \leq 16$ ) below and in the region of the stability threshold ( $E_{\text{stab}}$ ), and also the effective numbers of nucleons  $N_{\text{eff}}^{n(p)}$ , are given in Tables I–V. In the first column, we give the symbols of the hypernuclei, and in the second the lowest thresholds (neutron ( $n$ ), proton ( $p$ ), deuteron ( $d$ ), triton ( $t$ ),  $\alpha$ -particle, or  $\Lambda$ -hyperon) of disintegration of the hypernucleus and their energies. In the third column, we give the energies ( $E_N$ ) and quantum numbers ( $J_N, T_N$ ) of the levels of the nuclear core. In the fourth column we give  $N_{\text{eff}}^{n(p)}$  calculated for both transitions with spin flip (SF) and without it (NSF) in the weak-binding limit. The effective numbers depend weakly on the choice of the  $\Lambda N$  interaction and are largely determined by the spectroscopic factors of the target nucleus.<sup>58</sup> In the following columns, we give the energies of the hypernuclear levels calculated with the parameter sets given in Table VI. The calculations with the standard set ST were made with Cohen–Kurath



TABLE II. Spectra of levels of the hypernuclei  ${}^{11}_{\Lambda}\text{B}$ ,  ${}^{12}_{\Lambda}\text{C}$ ,  ${}^{13}_{\Lambda}\text{C}$ , lowest disintegration thresholds, and effective neutron numbers  $N_{\text{eff}}^n$ .

$A_Z$	$E_{\text{stab}},$ MeV	$E_N,$ MeV	$J_{NTN}$	$N_{\text{eff}}^n \%$		$J$	SG	SL	ST	KSA	IMB [131]
				NSF	SF						
${}^{11}_{\Lambda}\text{B}$	7,71 (p)	0	3 0	29	7 22	5/2 7/2	0 0,16	0 0,08	0 0,25	0 0,5	0 0,26
		0,72	1 0	13 4	11 6	3/2 1/2		0,83 1,02	1,12 0,62	0,97 1,09	0,96 0,75
		5,16	2 1	18 1	4 15	3/2 5/2		5,30 5,32	5,34 5,38	—	—
${}^{12}_{\Lambda}\text{C}$	9,8 (p)	0	3/2 1/2	71	12 59	1 2	0 0,08	0 0,04	0 0,086	0 0,15	0 0,14
		2,00	1/2 1/2	19	6 13	0 1	2,14 2,15	2,26 2,40	2,12 2,19	{ 2,33 2,17	1,83 1,75
		4,80	3/2 1/2	9	8 1	2 1	4,96 5,04	5,25 5,39	4,94 5,12	{ 5,24 4,90	4,91 4,90
${}^{13}_{\Lambda}\text{C}$	11,69 ( $\Lambda$ )	0	0 0	12	12	1/2	0	0	0	0	0
		4,44	2 0	23	5 18	3/2 5/2	4,51 4,51	4,68 4,72	4,49 4,50	4,42 4,46	4,60 4,62
		10,3	0 0	4	4	1/2	10,31	10,42	10,25		12,21
		15,11	1 1	12 1	2 11	1/2 3/2	15,02 15,15	15,09 15,14	14,96 15,15		15,11
		16,11	2 1	20	4 16	3/2 5/2	16,03 16,11	15,97 16,10	15,99 16,13		16,51

nuclear wave functions. The sets SG and SL were used in calculations of the spectra of hypernuclei with  $11 \leq A \leq 15$  with Cohen-Kurath nuclear wave functions, while the spectra of the hypernuclei with  $7 \leq A \leq 10$  were calculated with these sets using Barker's nuclear wave functions.

In the final columns of Tables I–III we give results obtained with central  $\Lambda N$  potentials in the shell model (KSA<sup>120</sup> and IMB<sup>131</sup>) and in the cluster model for  ${}^7_{\Lambda}\text{Li}(ad\Lambda)$ ,  ${}^8_{\Lambda}\text{Li}(at\Lambda)$ , and  ${}^9_{\Lambda}\text{Be}(aa\Lambda)$  (WBT<sup>87</sup>).

In Ref. 120, nuclear wave functions in intermediate coupling<sup>132</sup> were used, and the matrix element  $\Delta$  was calculated with a  $\Lambda N$  potential as a sum of two Gaussian functions whose intensity was chosen on the basis of the energy (0.79 MeV) of the  $3^+ / 2$  level in  ${}^7_{\Lambda}\text{Li}$  (Ref. 110), which was not confirmed in subsequent experiments. Allowance was made for the changes in the values of  $\Delta$  due to the differences between the binding energies of the  $\Lambda$  hyperon and the nuclear density. In contrast to Ref. 120, the calculations of Ref. 131 were based on the Cohen-Kurath nuclear wave functions, and the parameter  $\Delta$  was calculated with oscillator functions (oscillator parameter  $r_{0N(\Lambda)} = \sqrt{\hbar / M_{N(\Lambda)} \omega}$  and  $\hbar \omega = 41.0 / A^{1/3}$ ) and the  $\Lambda N$  potential YNG [the potential YNG was obtained in Ref. 4 by Brueckner's method on the basis of the free  $\Lambda N$  interaction of the Nijmegen group (model *D*, Ref. 79) corrected on the basis of the doublet splitting of the  $1^+$  and  $0^+$  levels in  ${}^4_{\Lambda}\text{H}$  ( ${}^4_{\Lambda}\text{He}$ )].

The calculations in the cluster model were made with two forms of the  $\Lambda N$  potential: YNG and ORG [Gaussian

potential with spin dependence  $V(r)(1 + \eta \sigma_{\Lambda} \sigma_N)$ ; the values  $\eta = -0, 1$  were chosen from the description of hypernuclear resonances in  $(K^-, \pi^-)$  reactions with a  $\Lambda$  hyperon in the  $1p$  state.<sup>133</sup> The variants *L* and *S* correspond to a long- and short-range (ordinary) spin-orbit ( $\alpha$ - $d$ ) interaction.

Particularly interesting for experiments in this level systematics are hypernuclear states that can be strongly excited ( $N_{\text{eff}} = W \gtrsim 10$ –15%) in reactions without and with spin flip and then emit  $\gamma$  rays in subsequent radiative transitions. We recall that we have in mind here the non-spin-flip reactions  $(K^-, \pi^-)$ ,  $(\pi^+, K^+)$  ( ${}^A_{\Lambda}\text{Z}$  in Tables I–III) and  $(K^-, \pi^0)$  ( ${}^A_{\Lambda}\text{Z}$  in Tables IV–V) at small emission angles of the  $\pi^0$  and  $K^+$  mesons and the spin-flip reaction  $(\pi^+, K^+)$  at  $\theta_k \gtrsim 10^\circ$  and  $(\gamma, K^0)$  ( ${}^A_{\Lambda}\text{Z}$  in Tables I–III).

Among the ground-state doublets, only the states  ${}^7_{\Lambda}\text{Li}$  ( $3^+ / 2$ ; 440 keV,  $W=35\%$ , spin flip);  ${}^{11}_{\Lambda}\text{B}$  ( $7^+ / 2$ ; 120–160 keV,  $W=22\%$ , spin flip) (variant SG in Tables I–II):

${}^9_{\Lambda}\text{Li}$  ( $5^+ / 2$ ; 280 keV,  $W=40\%$ , spin flip) (Table IV);  ${}^{13}_{\Lambda}\text{B}$  ( $3^+ / 2$ ; 130 keV,  $W=25\%$ , spin flip) (Table V)

can give  $\gamma$  rays of the corresponding energies. There can also be  $\gamma$  deexcitation of the  $2_1^-$  level in  ${}^8_{\Lambda}\text{Li}$  (300 keV), but this hypernucleus can be produced only as a result of baryonic decays of hypernuclear resonances. The upper components of the other doublets are isomer states and must decay by virtue of the weak interaction through the mesonic and mesonless channels. In addition, no  $\gamma$  lines are expected from the lightest hypernuclei of the  $1p$  shell with

TABLE III. Spectra of levels of the hypernuclei  ${}^{14}_{\Lambda}\text{N}$ ,  ${}^{15}_{\Lambda}\text{N}$ ,  ${}^{16}_{\Lambda}\text{O}$  and effective neutron numbers  $N_{\text{eff}}^n$ . For  ${}^{16}_{\Lambda}\text{O}$  the result obtained with the set SG(10, 16) is given in the brackets.

$\begin{smallmatrix} A \\ Z \end{smallmatrix}$ ${}^A_{\Lambda}Z$	$E_{\text{stab}}$ MeV	$E_N$ , MeV	$J_N T_N$	$N_{\text{eff}}^n$ %		$J$	SG	SL	ST	KSA	IMB
				NSF	SF						
${}^{14}_{\Lambda}\text{N}$	2,42 (p)	0	1/2 1/2	6 8	3 11	0 1	0 0,012	0 0,16	0 0,051	$\begin{Bmatrix} 0,43 \\ 0 \end{Bmatrix}$	0,08 0
${}^{15}_{\Lambda}\text{N}$	8,97 (p)	0	1 0	23 1	15 9	3/2 1/2	0 0,04	0,18 0	0 0,014	$\begin{Bmatrix} 0,31 \\ 0 \end{Bmatrix}$	0 0,63
		2,32	0 1	7	7	1/2	2,38	2,58	2,37	2,54	2,68
		3,95	1 0	12	3 9	1/2 3/2	3,89 4,24	4,42 4,71	3,72 4,29	3,98 4,58	3,75 4,35
		7,03	2 0	21	4 17	3/2 5/2	7,10 7,22	7,53 7,71	7,03 7,18	7,19 7,31	7,21 7,29
		9,17	2 1	20	4 16	3/2 5/2	9,3 9,36	9,75 9,87	9,25 9,36	9,16 9,56	9,80
${}^{16}_{\Lambda}\text{O}$	$\sim 7,5$ (p)	0	1/2 1/2	33	11 22	0 1	0 0,02 (0,09)	0 0,18	0 0,084	—	—
		6,18	3/2 1/2	67	11 56	1 2	6,27 6,41	6,77 6,88	6,26 6,46	—	—

$A=6$ ; for the hypernucleus  ${}^6_{\Lambda}\text{Li}$  is unstable with respect to decay through the channel  $p + {}^5_{\Lambda}\text{He}$ , and although the  $(2_1^-, 1^-)$  splitting in  ${}^6_{\Lambda}\text{He}$  is less than the threshold energy of the  $n + {}^5_{\Lambda}\text{He}$  channel ( $0.24 \pm 0.10$  MeV), the  $2_1^-$  level, which is strongly excited in spin-flip reactions ( $W=50\%$ ), is an isomer level.

Appreciably more  $\gamma$  lines in  $1p$ -shell hypernuclei are expected from below-threshold hypernuclear states formed on excited nuclear levels. An exception is the  $5^+/2$  level (1.81 MeV,  $W=30\%$ , non-spin-flip;  $W=17\%$ , spin-flip) in  ${}^7_{\Lambda}\text{He}$ . Owing to the presence of two neutrons in the  $1p$  shell, the rate of the  $E2$  transition  $5^+/2 \rightarrow 1^+/2$  in this hypernucleus is much less than the rate of weak decay of the  $\Lambda$  hyperon ( $\tau_{\Lambda}^{-1} \approx 4 \times 10^9 \text{ sec}^{-1}$ ). Moreover, the rate of the  $M1$  transition  $5^+/2 \rightarrow 3^+/2$  is also, owing to the nearly equal energies of these levels, appreciably less ( $\approx 1.2 \times 10^8 \text{ sec}^{-1}$ ) than  $\tau_{\Lambda}^{-1}$ , i.e., the  $5^+/2$  level must be an isomer. The existence in  ${}^7_{\Lambda}\text{He}$  of an isomer state is indicated by emulsion data—for this hypernucleus, an unusually broad distribution of the  $\Lambda$ -hyperon binding energy is observed.<sup>134</sup> In the spin-flip  $(\gamma, K^+)$  reaction on  ${}^7\text{Li}$  observation of the  $M1$   $\gamma$  transition  $3^+/2$  (1.8 MeV,  $W=16\%$ , spin-flip)  $\rightarrow 1^+/2$  (ground state) is possible. Electromagnetic transitions in  ${}^7_{\Lambda}\text{Li}$  and  ${}^7_{\Lambda}\text{He}$  were discussed in detail from the theoretical point of view in Ref. 135 under different assumptions about the energies of the levels.

In the scheme of  ${}^7_{\Lambda}\text{Li}$  levels adopted here, one can, in addition to the  $\gamma$  transition  $5^+/2$  (2.07 MeV,  $W=30\%$ , non-spin-flip)  $\xrightarrow{E2} 1^+/2$  (ground state) already discovered

in the  $(K^-, \pi^-, \gamma)$  reaction,<sup>5)</sup> expect  $\gamma$  lines in the spin-flip  $(\pi^+, K^+, \gamma)$  or  $(\gamma, K\gamma')$  reactions with energies  $E_{\gamma} = 1.86$  MeV and  $E_{\gamma} = 0.44$  MeV in the successive  $\gamma$  transitions  $7^+/2$  (2.30 MeV,  $W=23\%$ , spin-flip)  $\xrightarrow{E2} 3^+/2_1$

$\xrightarrow{M1} 1^+/2$  (ground state). The transition  $7^+/2 \xrightarrow{E4, M3} \rightarrow 1^+/2$  (ground state) is suppressed because of the higher multipolarity of the  $\gamma$  radiation. In our calculations, the level  $(1^+/2, 1; 3.64 \text{ MeV})$  in  ${}^7_{\Lambda}\text{Li}$  is found to be bound. It can be excited in spin-flip and non-spin-flip reactions with equal probabilities of about 14%. In the deexcitation of the  $(1^+/2, 1)$  state the  $\gamma$  transitions  $(1^+/2; 1) \xrightarrow{M1} (3^+/2, 0)$  and  $(1^+/2, 1) \xrightarrow{M1} (1^+/2, 0)$  with emission

of  $\gamma$  rays with energies of about 3.2 and 3.64 MeV are dominant. It may be assumed that these  $\gamma$  lines were not noted in the experiment of Ref. 37 because of the low intensity of excitation of the  $(1^+/2, 1)$  level and the reduced sensitivity of the detection apparatus in this region of the  $\gamma$  spectra. Note that direct observation of the  $\gamma$  transition  $3^+/2_1$  (0.44 MeV)  $\rightarrow 1^+/2$  (ground state) in  ${}^7_{\Lambda}\text{Li}$  is great interest for confirming the reliability of identification of the secondary hypernuclear  $\gamma$  ray in the decay  ${}^{10}_{\Lambda}\text{B}^* \rightarrow {}^3\text{He} + {}^7_{\Lambda}\text{Li}^*$  (Refs. 111 and 112).

In the hypernucleus  ${}^{11}_{\Lambda}\text{B}$ , the intensities of the different types of excitation (with and without spin flip) with  $W \approx 10\text{--}20\%$  are distributed over pairs of levels:  $3^+/2_1$  (0.83

TABLE IV. Spectra of levels of the hypernuclei  ${}^7_{\Lambda}\text{He}$ ,  ${}^9_{\Lambda}\text{Li}$ ,  ${}^{10}_{\Lambda}\text{Be}$ , and  ${}^{11}_{\Lambda}\text{Be}$  and effective proton numbers  $N_{\text{eff}}^p$ .

$\begin{smallmatrix} A \\ \Lambda \end{smallmatrix} Z$	$E_{\text{stab}}, \text{ MeV}$	$E_N, \text{ MeV}$	$J_N T_N$	$N_{\text{eff}}^p, \%$		$J$	SL	ST
				NSF	SF		$E, \text{ MeV}$	
${}^7_{\Lambda}\text{He}$	2,84 (n)	0	0 1	56	56	1/2	0	0
		1,80	2 1	3 30	16 17	3/2 5/2	1,80 1,81	1,77 1,82
${}^9_{\Lambda}\text{Li}$	3,76 (n)	0	2 1	50	10 40	3/2 5/2	0 0,28	0 0,52
		0,98	1 1	22	10 12	1/2 3/2	1,27 1,25	1,25 1,35
		2,25	3 1	18	4 14	5/2 7/2	2,27 2,47	— —
${}^{10}_{\Lambda}\text{Be}$	4,07 (n)	0	3/2 1/2	18	9 9	1 2	0 0,06	0 0,17
		2,49	5/2 1/2	4 14	9 9	2 3	2,50 2,59	2,38 2,54
${}^{11}_{\Lambda}\text{Be}$	$\sim 7,9$ (n)	0	0 1	13	13	1/2	0	0
		3,60	2 1	48 3	11 40	3/2 5/2	3,49 3,51	3,0 3,44

MeV,  $W=13\%$ ),  $3^+/2_2$  (5.3 MeV,  $W=18\%$ ) (non-spin-flip) and  $3^+/2_1$  (0.83 MeV,  $W=11\%$ ),  $5^+/2_2$  (5.32 MeV,  $W=15\%$ ) (spin-flip). Therefore, besides  $\gamma$  lines with low energies, 0.75 and 0.83 MeV, and  $\gamma$  rays of the maximal energy 5.3 MeV, there may be a number of cascade  $\gamma$  transitions, and this may complicate their identification.

The calculated excitation intensity of the doublet ( $5^+/2$ , spin-flip;  $3^+/2$ , non-spin-flip) in  ${}^{13}_{\Lambda}\text{C}$  is 20%. Since it is comparable with the excitation intensity of the ( $3^+/2, 5^+/2$ ) doublet in  ${}^9_{\Lambda}\text{Be}$ , the  $\gamma$  line from which has already been detected in the ( $K^-, \pi^- \gamma$ ) reaction, one can also hope for detection of a  $\gamma$  line in  ${}^{13}_{\Lambda}\text{C}$  with  $E_{\gamma} \simeq 4.5$  MeV.

A very interesting possibility for testing the "purity" of isospin in hypernuclei is the search for  $\gamma$  rays in  ${}^{13}_{\Lambda}\text{C}$  with  $E_{\gamma} = 15\text{--}16$  MeV from deexcitation of doublets with isospin  $T=1$ , namely, ( $3^+/2_2$ , 15.15 MeV,  $W=11\%$ , spin-flip;  $1^+/2_3$ , 15.02 MeV,  $W=12\%$ , non-spin-flip); ( $5^+/2_2$ , 16.11 MeV,  $W=16\%$ , spin-flip;  $3^+/2_3$ , 16.03 MeV,  $W=20\%$ , non-spin-flip), formed on the states  ${}^{12}\text{C}$   $1^+$ ,  $1$  (15.11 MeV) and  $2^+$ ,  $1$  (16.11 MeV) and lying appreciably above the thresholds of the channels  $\Lambda + {}^{12}\text{C}$  ( $\approx 11.69$  MeV) and  $\alpha + {}^9_{\Lambda}\text{Be}$  ( $\approx 12.35$  MeV) but near the threshold of the proton decay channel  $p + {}^{12}_{\Lambda}\text{B}$  ( $\approx 16.08\text{--}16.44$  MeV).<sup>30,45</sup> The ratio of the radiative and baryonic decay probabilities for the ( $1^+/2_3$ , 1) level of  ${}^{13}_{\Lambda}\text{C}$  was estimated in Ref. 136.

In  ${}^{14}_{\Lambda}\text{N}$ , a yield of primary  $\gamma$  rays is not expected, since

in this hypernucleus excitations in the continuous spectrum are dominant. Secondary  $\gamma$  rays are expected from the hypernucleus  ${}^{13}_{\Lambda}\text{C}$  (4.4 MeV), which is formed by proton decay of  ${}^{14}_{\Lambda}\text{N}$  with  $E \geq 7$  MeV (Ref. 43). Because of the high stability threshold and strong fragmentation of the excitations in the energy region up to  $\approx 9$  MeV in  ${}^{15}_{\Lambda}\text{N}$ , as in  ${}^{11}_{\Lambda}\text{B}$ , a whole series of  $\gamma$  rays can be emitted, especially in  $\gamma$  deexcitation of the doublet ( $5^+/2_1, 3^+/2_3$ ) ( $W=21\%$ ), which is situated in the region of 7 MeV.

The hypernucleus  ${}^{16}_{\Lambda}\text{O}$  is characterized by high probabilities for excitation of the doublet ( $1_2^-, 6.27$  MeV,  $W=67\%$ , non-spin-flip); ( $2_1^-, 6.41$  MeV,  $W=56\%$ , spin-flip). The  $2_1^-$  level must decay mainly through the  $M1$   $\gamma$  transition to the  $1_1^-$  isomer state. The  $W_{\gamma}(1_2^- \rightarrow 1_1^-)/W_{\gamma}(1_2^- \rightarrow 0^-)$  probability ratio is 2.8. In the region of energies (5 MeV) between the ( $1^-, 0^-$ ) and ( $2^-, 1^-$ ) doublets there are positive-parity states of  ${}^{16}_{\Lambda}\text{O}$ , namely,  $0^+$ ,  $1^+$ ,  $2^+$ , and  $3^+$ , formed on the  ${}^{15}\text{O}$  states  $1^+/2$  (5.18 MeV) and  $5^+/2$  (5.24 MeV) (intruder states).<sup>82</sup> However, because the probability of  $\gamma$  deexcitation of the level  $3^-/2$  (6.18 MeV) to  $1^-/2$  in  ${}^{15}\text{N}$  ( ${}^{15}\text{O}$ ) is  $\approx 99\%$ , the  $0^+$ ,  $1^+$ ,  $2^+$  states in  ${}^{16}_{\Lambda}\text{O}$  ( ${}^{16}_{\Lambda}\text{N}$ ) will have practically no participation in the  $\gamma$  transitions between the doublet states of negative parity in these hypernuclei. However, as was noted in Ref. 74, such states can be directly excited in ( $K^-, \pi^-$ ) and other reactions because of the admixture of ( $2h\text{--}2p$ ) configurations in the  ${}^{16}\text{O}$  target nucleus. Observation of  $\gamma$  rays in  ${}^{16}_{\Lambda}\text{O}$  ( ${}^{16}_{\Lambda}\text{N}$ ) with

TABLE V. Spectra of levels of the hypernuclei  ${}_{\Lambda}^{12}\text{B}$ ,  ${}_{\Lambda}^{13}\text{B}$ ,  ${}_{\Lambda}^{14}\text{C}$ ,  ${}_{\Lambda}^{15}\text{C}$ , and  ${}_{\Lambda}^{16}\text{N}$  and effective proton numbers  $N_{\text{eff}}^p$ .

$A_Z$	$E_{\text{stab}}, \text{MeV}$	$E_N, \text{MeV}$	$J_N T_N$	$N_{\text{eff}}^p, \%$		$J$	SG	ST
				NSF	SF		$E, \text{MeV}$	
${}_{\Lambda}^{12}\text{B}$	11,37 ( $\Lambda$ )	0	3/2 1/2 <sub>s</sub>	71	12 59	1 2	0 0,06	0 0,09
		2,12	1/2 1/2	19	6 13	0 1	2,26 2,27	2,24 2,31
${}_{\Lambda}^{13}\text{B}$	~ 3,7 ( $n$ )	0	1 1	25 5	5 25	1/2 3/2	0 0,13	0 0,19
		0,95	2 1	50	10 40	3/2 5/2	0,96 1,05	1,04 1,17
${}_{\Lambda}^{14}\text{C}$	5,43 ( $n$ )	0	1/2 1/2	6 8	3 11	0 1	0 0,012	0 0,05
${}_{\Lambda}^{15}\text{C}$	~ 8,9 ( $n$ )	0	0 1	17	17	1/2	0	0
		7,01	2 1	48	10 38	3/2 5/2	6,92 6,98	6,92
${}_{\Lambda}^{16}\text{N}$	~ 11 ( $n$ )	0	1/2 1/2	33	11 22	0 1	0 0,02	0 0,08
		6,32	3/2 1/2	67	11 56	1 2	6,41 6,55	6,4 6,6

$E_\gamma \simeq 5 \text{ MeV}$  would indicate realization of such processes.

Tables IV and V give the spectra and  $N_{\text{eff}}^n$  for hypernuclear states that can be formed in single-nucleon ( $K^-, \pi^0$ ) or ( $\gamma, K^+$ ) reactions (non-spin-flip or spin-flip excitations) on the protons of target nuclei. The spectra,  $N_{\text{eff}}^{n(p)}$ , yields, and energies of the expected  $\gamma$  rays in the hypernuclei with even  $A$  (isospin  $T=1/2$ ) in Tables I–III and IV–V must be the same because of the isospin symmetry of the baryon–baryon interactions. Only the stability thresholds for these hypernuclei are different. Breaking of the isospin symmetry can be manifested in differences of the corresponding energies of the  $\gamma$  transitions in pairs of hypernuclei with the same  $A$  produced in reactions on neutrons (protons) of target nuclei with  $N=Z$ .

All hypernuclei with odd  $A$  produced in reactions on targets with  $T=1/2$  have isospin  $T=1$ . In the hypernucleus  ${}_{\Lambda}^9\text{Li}$  there is, in addition to strong excitation of the levels of the ground-state doublet ( $5^+/2, 3^+/2$ ) ( $W \simeq 40\text{--}50\%$ ), an appreciable probability ( $W \simeq 14\text{--}22\%$ ) for excitation of the doublets ( $3^+/2, 1^+/2_1$ ) and ( $7^+/2, 5^+/2_2$ ), the  $\gamma$  deexcitation of which gives a series of  $\gamma$  cascade lines with maximum energy  $\simeq 2.5 \text{ MeV}$ . In other hypernuclei,  ${}_{\Lambda}^{11}\text{Be}$ ,  ${}_{\Lambda}^{13}\text{Be}$ ,  ${}_{\Lambda}^{13}\text{B}$ , and  ${}_{\Lambda}^{15}\text{C}$ , excitation of the doublet ( $5^+/2$ , spin-flip;  $3^+/2$ , non-spin-flip) ( $W = 40\text{--}50\%$ ) is dominant. In  ${}_{\Lambda}^{11}\text{Be}$  and  ${}_{\Lambda}^{15}\text{C}$  one  $\gamma$  line is expected for each type of excitation (without or with spin flip), their energies being  $E_\gamma \simeq 3.5 \text{ MeV}$  and  $E_\gamma \simeq 7 \text{ MeV}$ , respectively. In  ${}_{\Lambda}^{13}\text{B}$ , deexcitation of the  $3^+/2_2$  level can give rise to cascade  $M1$   $\gamma$  transitions through the interme-

diate level  $3^+/2_1$ , and also the direct  $\gamma$  transition  $3^+/2_2 \xrightarrow{M1} 1^+/2$  (ground state). The ratio of the transition probabilities is  $W_\gamma(3^+/2_2 \rightarrow 3^+/2_1)/W_\gamma(3^+/2 \rightarrow 1^+/2) = 0.15$ . The rate of the  $\gamma$  transition  $3^+/2_1 \rightarrow 1^+/2$  is  $1.7 \times 10^{10} \text{ sec}^{-1}$ . Deexcitation of the level  $5^+/2$  is realized in the  $\gamma$  cascade transitions  $5^+/2 \xrightarrow{M1} 3^+/2 \xrightarrow{M1} 1^+/2$ .

The doublet splittings of the hypernuclear levels calculated in Refs. 87 and 120 with central  $\Lambda N$  potentials (seventh and eighth columns of Tables I–III) are appreciably greater than the splittings obtained in Ref. 38 and in our calculations.<sup>126</sup> The results of the calculations of Refs. 87 and 120 can evidently be brought closer to our results by reducing the intensity of the spin-dependent parts of the  $\Lambda N$  potentials. Note that in some doublets, identified by the curly brackets, a different order of the levels is obtained for the central  $\Lambda N$  forces.

#### Dependences of hypernuclear energy levels on the potential parameters of the shell model

As we have already said, we assume that the parameters of the shell model can, in general, depend on the mass number  $A$  and even on the quantum numbers of the individual hypernuclear levels. Therefore, the hypernuclear spectra given in Tables I–III and IV–V, found with model parameters made consistent with a restricted set of exper-

TABLE VI. Parameters of  $\Lambda N$  interaction used for calculating the level schemes of hypernuclei.

Type of interaction	$\Delta$	$s_{\Lambda}$	$s_N$	$T$
SG [126]	0,3	-0,02	-0,1 ( -0,35 for $_{\Lambda}^7\text{Li}$ )	0,02
SL [126]	0,3	-0,02	-0,35	0,04
ST [38]	0,5	-0,04	-0,08	0,04
SG (10, 16)* [126]	0,3	-0,025	-0,1	0,03

\*Interaction types alternative to SG for the hypernuclei  $^{10}_{\Lambda}\text{B}$  and  $^{16}_{\Lambda}\text{O}$ .

imental data on some levels of  ${}^7_\Lambda\text{Li}$ ,  ${}^9_\Lambda\text{Be}$ ,  ${}^{10}_\Lambda\text{B}$ ,  ${}^{12}_\Lambda\text{B}$ , and  ${}^{16}_\Lambda\text{O}$ , should be regarded as approximate for the time being. More information about hypernuclear  $\gamma$  transitions is needed to make the parameters more accurate.

Our analysis of the possible  $\gamma$  transitions in  $1p$ -shell hypernuclei shows that suitable target nuclei for looking for new hypernuclear  $\gamma$  lines in the reactions used in hypernuclear spectroscopy,  $(K^-, \pi^-)$  and  $(\pi^+, K^+)$ , could be  ${}^7\text{Li}$ ,  ${}^{13}\text{C}$ , and  ${}^{16}\text{O}$ . In some hypernuclei, for example,  ${}^8_\Lambda\text{Li}$ ,  $\gamma$  transitions can accompany nucleon or cluster decays of hypernuclear resonances in the continuous spectrum. For the low-lying states of  ${}^7_\Lambda\text{Li}$ ,  ${}^{13}_\Lambda\text{C}$ ,  ${}^{16}_\Lambda\text{O}$ ,  ${}^8_\Lambda\text{Li}$ ,  ${}^{11}_\Lambda\text{B}$ , which can give  $\gamma$  lines, Figs. 5 and 6 show the dependence of the level energies on the parameters  $\Delta$ ,  $S_\Lambda$ ,  $S_N$ , and  $T$  [see the

relation (33)]. The levels  $1_1^-$  in  ${}^{14}_\Lambda\text{N}$  and  $1^+ / 2_1$  in  ${}^{15}_\Lambda\text{N}$ , which are very weakly split ground-state doublets ( $1_1^-, 0^-$ ) and ( $1^+ / 2_1, 3^+ / 2$ ) and are very sensitive to the values of the parameters  $T$  and  $\Delta$ , are also shown in Fig. 6. The segment with an arrow at the top of each figure indicates the direction of increase of one of the parameters (for three parameters fixed) and simultaneously indicates the interval of values of the measured parameter with step  $h$ . In Figs. 5 and 6, the parameters were varied with step  $h$  in the following intervals: for  ${}^7_\Lambda\text{Li}$ :  $0.5 \geq \Delta \geq 0.1$  ( $h = 0.1$ ),  $0.02 \geq S_\Lambda \geq -0.06$  ( $h = 0.02$ ),  $-0.05 \geq S_N \geq -0.65$  ( $h = 0.15$ ),  $0.08 \geq T \geq 0$  ( $h = 0.02$ ); for  ${}^8_\Lambda\text{Li}$ ,  ${}^{11}_\Lambda\text{B}$ ,  ${}^{13}_\Lambda\text{C}$ ,  ${}^{14,15}_\Lambda\text{N}$ , and  ${}^{16}_\Lambda\text{O}$ :  $0.5 \geq \Delta \geq 0.1$  ( $h = 0.1$ ),  $0.02 \geq S_\Lambda \geq -0.06$  ( $h$

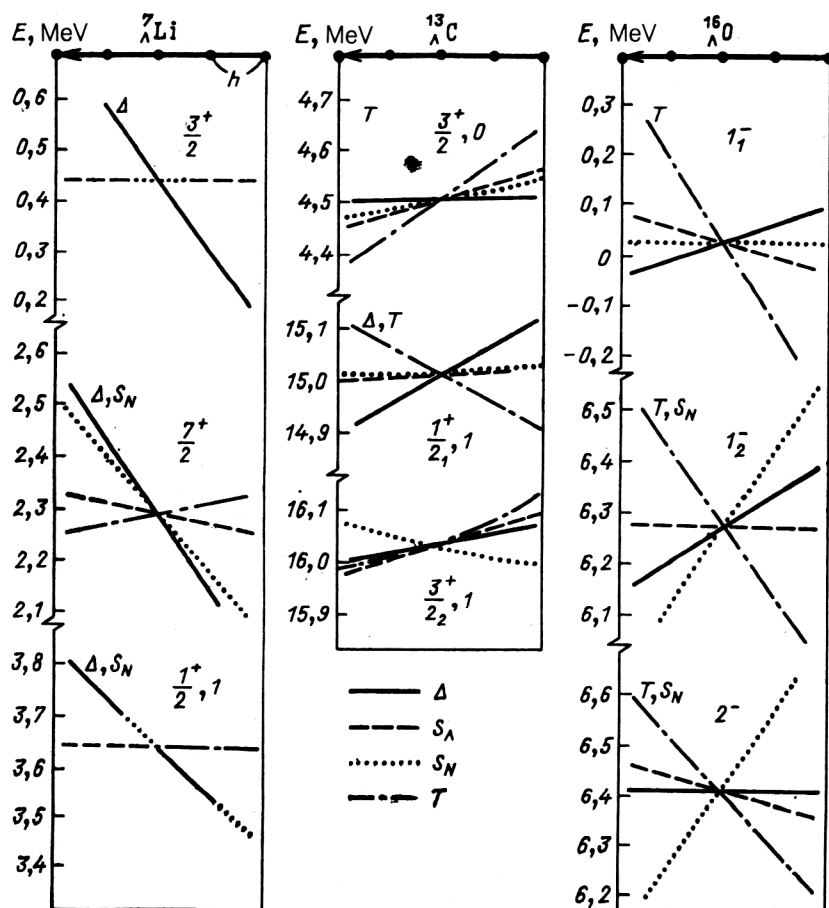


FIG. 5. Dependence of the energy levels of  ${}^7_\Lambda\text{Li}$ ,  ${}^{13}_\Lambda\text{C}$ , and  ${}^{16}_\Lambda\text{O}$  on the parameters  $\Delta$ ,  $S_\Lambda$ ,  $S_N$ , and  $T$ .



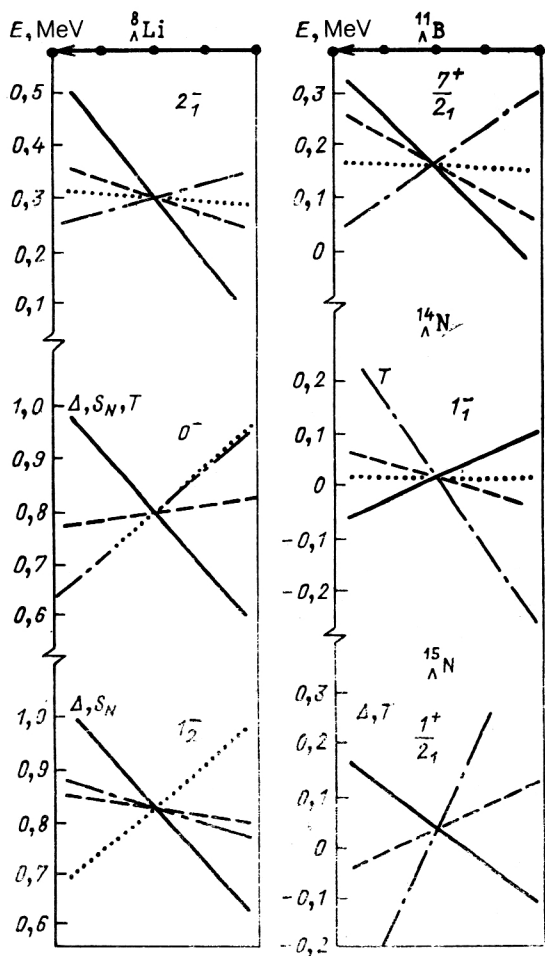


FIG. 6. Dependence of the energies of the levels of  ${}^8_\Lambda\text{Li}$ ,  ${}^{11}_\Lambda\text{B}$ ,  ${}^{14}_\Lambda\text{N}$ , and  ${}^{15}_\Lambda\text{N}$  on the parameters  $\Delta$ ,  $S_\Lambda$ ,  $S_N$ , and  $T$ .

$= 0.02$ ),  $0.1 \geq S_N \geq -0.3$  ( $h = 0.1$ ),  $0.06 \geq T \geq -0.02$  ( $h = 0.02$ ).

The parameters to which the individual hypernuclear levels shown in Figs. 5 and 6 are especially sensitive can be helpful in analysis of new experimental data.

## CONCLUSIONS

In this review we have presented the main features of the modern status of theoretical and experimental investigations in the spectroscopy of low-lying states of  $1p$ -shell hypernuclei. Besides discussing the various theoretical approaches to this problem, we have concentrated our attention on the shell description of hypernuclear states. The experience gained from the development of hypernuclear spectroscopy shows that the shell model, applied to hypernuclei, not only explains the existing experimental data but also gives new predictions that stimulate further experiments. This applies in the first place to bound (below-threshold) excited hypernuclear states, which are the subject of study in  $\gamma$  spectroscopy, and some states in the continuum, the experimental investigation of which promises to be quite interesting, for example, from the point of view of testing the "purity" of isospin in hypernuclei.

In the theory of the structure of light hypernuclei, we have concentrated the main attention on the results of the shell model with bound single-particle baryon states because from the technical point of view this approach is much simpler than the shell model that takes into account explicitly the continuous spectrum. However, it is known that these two approaches, at the first glance very different, often give similar results.<sup>59</sup> Of course, it could be that the accumulation of detailed data on hypernuclear states in the continuum will require introduction of a continuous spectrum in the formalism of the shell model.

The main attention in this paper has been concentrated on the translationally invariant formulation of the shell model for hypernuclei developed by the authors—the TISM with oscillator wave functions of the baryons. This model has been developed by analogy with the TISM for ordinary nuclei. The advantage of the TISM appears in the possibility of giving a fairly simple description of the kinematic correlations that open the baryonic decay channels.

In a certain sense, the shell model of low-lying hypernuclear states with configuration  $\{s^4 p^n \otimes s_\Lambda\}$  is even simpler than the shell model of ordinary nuclei. For the two-particle  $\Lambda N$  interaction, there are just five potential parameters,  $\Delta$ ,  $S_\Lambda$ ,  $S_N$ ,  $T$ , and  $\bar{V}$ , whereas for the nuclear configuration  $\{s^4 p^n\}$  the total number of analogous parameters is more than ten. Unfortunately, there are as yet too few experimental data on hypernuclear spectra to draw definite conclusions about the values of the hypernuclear parameters (this applies especially to  $T$  and  $S_N$ ). A larger set of spectroscopic data would also permit a more reliable choice of ways to improve the hypernuclear models. Until recently, both the cluster and shell models described the  $\gamma$  transitions in  ${}^7_\Lambda\text{Li}$  and  ${}^9_\Lambda\text{Be}$  reasonably well, but recent measurements at BNL of the energies of the doublet splittings of the ground states in  ${}^{10}_\Lambda\text{B}$  and  ${}^{16}_\Lambda\text{O}$  required a correction in the parameters of the  $\Lambda N$  interaction of the shell model.<sup>126</sup> With the new parameters  $\Delta$ ,  $S_\Lambda$ ,  $S_N$ , and  $T$ , the predictions for the level energies calculated in the different approaches already differ appreciably, and measurements of the energies of excited hypernuclear levels become even more topical. Searches for deviations from the systematics of the spectra proposed with the new parameters are of great interest. It is not yet clear to what extent the most recent set of parameters  $\Delta$ ,  $S_\Lambda$ ,  $S_N$ , and  $T$  proposed in Ref. 126 is suitable for all  $1p$ -shell hypernuclei. In principle, the universality could be lost through the influence of three-particle  $\Lambda NN$  forces, the cluster structure of individual hypernuclei, coupling of the  $\Lambda$  and  $\Sigma$  channels in the hyperon-nucleon interaction, and other effects. We hope that all these questions will be gradually clarified as spectroscopic data on hypernuclei are accumulated.

Besides the  $(K^-, \pi^0 \gamma)$  reactions, which hardly affect the spin degrees of freedom, an important role in the solution of all these problems will be played by  $(\pi^+, K^+ \gamma)$ ,  $(\gamma, K^+)$ , and  $(e, e' K^+)$  processes, in which spin excitations (reactions with spin flip) must be manifested. Investigations in the  $\gamma$  spectroscopy of hypernuclei with neutron excess, produced in single-nucleon reactions on protons of target nuclei, will introduce new features.

It is clear from our exposition that to test the models of hypernuclear structure and the various forms of hyperon-nucleon interaction that have been considered it is necessary to perform further appropriate experiments in the spectroscopy of hypernuclei and, in particular,  $\gamma$  spectroscopy, the possibilities of which are far from exhausted. The shell model gives a good guide for new investigations in this field.

We have considered here hypernuclear  $\gamma$  transitions from low-lying states that arise in the primary reactions of hypernuclear production. Baryonic decays of hypernuclear resonances may be accompanied by electromagnetic transitions in daughter hypernuclei, the discussion of which is deferred until part II of the review.

We should like to express our great debt to our friend Professor Marion Gmitro, whose untimely death occurred in October 1990, for exceptional interest in the work and widespread support for Czechoslovak-Soviet collaboration, without which it would have been impossible to carry out the extended series of joint studies on hypernuclear spectroscopy. We are sincerely grateful to Academician A. M. Baldin for constant support of our investigations in the physics of hypernuclei at the P. N. Lebedev Physics Institute and the Institute of Nuclear Research of the USSR Academy of Sciences.

We should like to take this opportunity of thanking Professor R. E. Chrien of the Brookhaven National Laboratory for communicating experimental data on the search for  $\gamma$  transitions in hypernuclei before their publication.

- <sup>1)</sup>Recent studies at the National Laboratory of High Energy Physics (KEK, Japan) found indications in the  $(K^-, \pi^-)$  reaction on  ${}^4\text{He}$  of the existence of a bound state of  $\Sigma$  hyperons with three nucleons.<sup>19</sup> These data have revived interest in the problem of  $\Sigma$  hypernuclei.<sup>20</sup>
- <sup>2)</sup>Experimental data on the spectroscopic factors can be found in the references of Ref. 58.
- <sup>3)</sup>The study of Ref. 122 used eight values of  $B_\lambda$  for hypernuclei with mass numbers  $8 \leq A \leq 13$  (1968 data), whereas the calculations in Refs. 72 and 74 included 12 values of  $B_\lambda$  for  $A = 5.7 \leq A \leq 15$  (1974 data).
- <sup>4)</sup>With Cohen-Kurath nuclear wave functions the value  $S_N = -0.2$  is obtained for  ${}^7_\Lambda\text{Li}$ ; this differs from the  $S_{N\text{stand}}$  in (40), adopted on the basis of the estimate  $-0.17 \leq S_N \leq -0.043$  of Ref. 38 on the basis of the free  $\Lambda N$  interaction in model  $D$  of the Nijmegen group.<sup>79</sup>
- <sup>5)</sup>The competing  $\gamma$  transition  $5^+ / 2^- \rightarrow 3^+ / 2^-$  with  $E_\gamma = 1.63$  MeV was not observed because of the small ratio of the transition probabilities:  $W_\gamma(5^+ / 2^- \rightarrow 3^+ / 2^-) / W_\gamma(5^+ / 2^- \rightarrow 1^+ / 2^-) = 0.14$ .
- <sup>1)</sup>J. Pniewski, *Methods in Subnuclear Physics*, edited by M. Nikolic, Vol. 5, Part 1 (Gordon and Breach, New York, 1969), p. 457; G. Bohm and U. Kreckler, *Fiz. Elem. Chastits At. Yadra* 3, 318 (1972) [*Sov. J. Part. Nucl.* 3, 162 (1972)]; B. A. Khrylin, *Usp. Fiz. Nauk* 105, 185 (1971) [*Sov. Phys. Usp.* 14, 616 (1971)].
- <sup>2)</sup>A. Gal, *Adv. Nucl. Phys.* 8, 1 (1975); B. Povh, *Prog. Part. Nucl. Phys.* 5, 245 (1981); L. N. Bogdanova and V. E. Markushin, *Fiz. Elem. Chastits At. Yadra* 15, 808 (1984) [*Sov. J. Part. Nucl.* 15, 361 (1984)]; V. N. Fetisov, Preprint No. 340 [in Russian], P. N. Lebedev Physics Institute, Moscow (1987).
- <sup>3)</sup>C. B. Dover and G. E. Walker, *Phys. Rep.* 89, 1 (1982).
- <sup>4)</sup>Structure of Hypernuclei, *Prog. Theor. Phys. Suppl.* No. 81 (1985).
- <sup>5)</sup>R. E. Chrien and C. B. Dover, *Ann. Rev. Nucl. Part. Sci.* 39, 113 (1989).
- <sup>6)</sup>M. I. Podgoretski, *Zh. Eksp. Teor. Fiz.* 44, 695 (1963) [*Sov. Phys. JETP* 17, 470 (1963)]; H. J. Lipkin, *Phys. Rev. Lett.* 14, 18 (1965); H. Feshbach and A. K. Kerman, *Preludes in Theoretical Physics*, edited by

- A. de Shalit, H. Feshbach, and L. Van Hove (North-Holland, Amsterdam, 1965), p. 260; A. K. Kerman and H. J. Lipkin, *Ann. Phys.* (N.Y.) 66, 738 (1971).
- <sup>7)</sup>*Proc. of the Seminar on the Kaon-Nucleus Interaction and Hypernuclei, Zvenigorod, September 12-14, 1977* [in Russian] (Nauka, Moscow, 1979).
- <sup>8)</sup>*Proc. of the 1979 Intern. Conf. on Hypernuclei and Low Energy Kaon Physics*, Vol. 25 (Nukleonika, 1980), Nos. 3-4.
- <sup>9)</sup>*Proc. of the Intern. Conf. on Hypernuclei and Kaon Physics*, edited by B. Povh (Heidelberg, June 20-24, 1982).
- <sup>10)</sup>*Proc. of the Intern. Conf. on Hypernuclei and Kaon Physics*, edited by R. E. Chrien (BNL, Upton, New York, Sept. 9-13, 1985); *Nucl. Phys.* A450, 1c (1986).
- <sup>11)</sup>*Proc. of the 1986 INS Intern. Symposium on Hypernuclear Physics*, edited by H. Bandō, O. Hashimoto, and K. Ogawa (Tokyo, August 20-23, 1986).
- <sup>12)</sup>*Contributed Papers at the 1986 INS Intern. Symposium on Hypernuclear Physics* (Tokyo, August 20-23, 1986).
- <sup>13)</sup>*Proc. of the Intern. Symposium on Hypernuclei and Low Energy Kaon Physics, Legnano*, edited by T. Bressani (Italy, Sept. 12-16, 1988); *Nuovo Cimento* 102A, 1 (1989).
- <sup>14)</sup>W. Brückner, B. Granz, D. Ingham *et al.*, *Phys. Lett.* 62B, 481 (1976); G. C. Bonazzola, T. Bressani, R. Cester *et al.*, *Phys. Lett.* 53B, 297 (1974); A. Bouyssy, see Ref. 8, p. 413; N. Bertini, O. Bing, P. Birien *et al.*, *Nucl. Phys.* A360, 315 (1981).
- <sup>15)</sup>R. Chrien, M. May, H. Palevsky *et al.*, *Phys. Lett.* 89B, 31 (1979); M. May, H. Piekarczyk, R. E. Chrien *et al.*, *Phys. Rev. Lett.* 47, 1106 (1981).
- <sup>16)</sup>R. Bertini, O. Bing, P. Birien *et al.*, *Phys. Lett.* 90B, 375 (1980); 136B, 29 (1984); 158B, 19 (1985); H. Piekarczyk, S. Bart, D. Hackenburg *et al.*, *Phys. Lett.* 110B, 428 (1982).
- <sup>17)</sup>A. Bouyssy, see Ref. 9, p. 11; L. Majling, M. Sotona, J. Žofka *et al.*, *Czech. J. Phys.* B36, 447 (1986); C. Dover, A. Gal, L. Klieb, D. J. Millener *et al.*, *Phys. Rev. Lett.* 56, 119 (1986).
- <sup>18)</sup>R. Wünsch and J. Žofka, *Phys. Lett.* 193B, 7 (1987); E. V. Hungerford, see Ref. 11, p. 6.
- <sup>19)</sup>R. S. Hayano, T. Ishikawa, M. Iwasaki *et al.*, see Ref. 13, p. 437.
- <sup>20)</sup>R. H. Dalitz, D. H. Davis, and A. Deloff, *Phys. Lett.* 236B, 76 (1990); T. Harada, S. Shinmura, Y. Akaishi, and H. Tanaka, *Nucl. Phys.* A507, 715 (1990); R. S. Hayano, *Nucl. Phys.* A508, 99c (1990).
- <sup>21)</sup>R. E. Chrien, *Nucl. Phys.* A478, 705c (1988); P. H. Pile, R. E. Chrien, S. Bart *et al.*, see Ref. 13, p. 413.
- <sup>22)</sup>T. Yamazaki, T. Ishikawa, M. Iwasaki *et al.*, see Ref. 10, p. 1; O. Hashimoto, see Ref. 11, p. 196.
- <sup>23)</sup>S. A. Avramenko, A. U. Abdurakhimov, V. D. Aksinenko *et al.*, *Pis'ma Zh. Eksp. Teor. Fiz.* 48, 477 (1988) [*JETP Lett.* 48, 519 (1988)]; A. U. Abdurakhimov, V. D. Aksinenko, M. H. Anikina *et al.*, see Ref. 13, p. 645.
- <sup>24)</sup>J. P. Bocquet, M. Rey-Campagnolle, G. Ericsson *et al.*, *Phys. Lett.* 182B, 146 (1986); 192B, 312 (1987); M. Rey-Campagnolle, see Ref. 13, p. 653; S. Polikanov, *Nucl. Phys.* A478, 805c (1988).
- <sup>25)</sup>V. I. Noga, Yu. N. Ranyuk, N. Ya. Rutkevich *et al.*, *Yad. Fiz.* 46, 1313 (1987) [*Sov. J. Nucl. Phys.* 46, 769 (1987)]; *Ukr. Fiz. Zh.* 35, 171 (1990).
- <sup>26)</sup>N. Z. Gogitidze, A. N. Eliseev, V. L. Kashevarov *et al.*, Preprint No. 22 [in Russian], P. N. Lebedev Physics Institute, Moscow (1980).
- <sup>27)</sup>K. Shoda, see Ref. 11, p. 184; C. Guaraldo, private communication.
- <sup>28)</sup>H. Ejiri, T. Fukuda, T. Shibata *et al.*, see Ref. 11, p. 223; M. Sotona, J. Žofka, H. Bandō, and V. N. Fetisov, *Czech. J. Phys.* B39, 1273 (1989).
- <sup>29)</sup>*Proc. of the Kaon Factory Workshop*, edited by M. K. Craddock, TRI-79-1 (Vancouver, August 13-14, 1979); *Physics with LAMPE II. Proposal*, June 1983, LA-9798-P, Los Alamos Nat. Lab. (1983); F. Bradamante, see Ref. 12; *Proposal, Japanese Hadron Project, INS Report Sept. (1987); Hypernuclear Physics at KAON, Proc. of the TRIUMF/KEK Workshop*, KEK Report 89-6 (June 17-18, 1989).
- <sup>30)</sup>Conceptual Design Report, CEBAF Basic Experimental Equipment, April 13, SURA, Newport News, Virginia (1990).
- <sup>31)</sup>C. Dover, L. Ludeking, and G. E. Walker, *Phys. Rev. C* 22, 2073 (1980).
- <sup>32)</sup>C. B. Dover, Preprint BNL-40074 (1987); T. Yamazaki, *INS-Rept.* 607, Oct. (1986); D. J. Millener, C. B. Dover, and A. Gal, *Phys. Rev. C* 38, 2700 (1988); T. Motoba, H. Bandō, R. Wünsch, and J. Žofka, *Phys. Rev. C* 38, 1322 (1988); Y. Yamamoto, H. Bandō, and S. Žofka, *Prog. Theor. Phys.* 80, 757 (1988).
- <sup>33)</sup>K. J. Nield, T. Bowen, G. D. Cable *et al.*, *Phys. Rev. C* 13, 1263

- (1976); R. Bowen, see Ref. 7, p. 115.
- <sup>34</sup>M. Wakai, H. Bandō, and M. Sano, Phys. Rev. C **33**, 748 (1988); H. Bandō, M. Sano, J. Žofka, and M. Wakai, Nucl. Phys. A**501**, 900 (1989); J. Žofka, M. Wakai, M. Sano, and H. Bandō, Phys. Lett. **235B**, 25 (1990).
- <sup>35</sup>V. A. Karnaukhov, see Ref. 7, p. 107.
- <sup>36</sup>A. S. Bychkov and R. U. Khafizov, Yad. Fiz. **48**, 65 (1988) [Sov. J. Nucl. Phys. **48**, 40 (1988)].
- <sup>37</sup>M. May, S. Bart, S. Chen *et al.*, Phys. Rev. Lett. **51**, 2085 (1983).
- <sup>38</sup>D. J. Millener, A. Cal, C. B. Dover, and R. H. Dalitz, Phys. Rev. C **31**, 499 (1985).
- <sup>39</sup>A. Bamberger, M. A. Faessler, U. Lynen *et al.*, Nucl. Phys. **B60**, 1 (1973).
- <sup>40</sup>M. Bedjidian, A. Filipkowski, J. Y. Grossiord *et al.*, Phys. Lett. **62B**, 467 (1976).
- <sup>41</sup>M. Bedjidian, E. Descroix, J. Y. Grossiord *et al.*, Phys. Lett. **83B**, 252 (1979).
- <sup>42</sup>L. Majling, M. Sotona, J. Žofka, V. N. Fetisov, and R. A. Eramzhyan, Phys. Lett. **92B**, 256 (1980); Preprint No. 205, FIAN (1980).
- <sup>43</sup>L. Majling, J. Žofka, V. N. Fetisov, and R. A. Eramzhyan, see Ref. 10, p. 189c.
- <sup>44</sup>J. Pniewski and D. Zieminska, see Ref. 7, p. 33.
- <sup>45</sup>R. Grace, P. D. Barnes, R. A. Eisenstein *et al.*, Phys. Rev. Lett. **55**, 1055 (1985); P. D. Barnes, see Ref. 10, p. 43c.
- <sup>46</sup>P. D. Barnes and J. L. Szymanski, see Ref. 11, p. 136.
- <sup>47</sup>R. H. Dalitz, Nucl. Phys. A**354**, 101c (1981).
- <sup>48</sup>J. Žofka, L. Majling, and V. N. Fetisov, see Ref. 12, p. 23; H. Bandō, T. Yamada, and J. Žofka, Phys. Rev. C **36**, 1640 (1987).
- <sup>49</sup>H. Tamura, T. Yamazaki, M. Sano *et al.*, Phys. Rev. C **40**, 479 (1989).
- <sup>50</sup>J. Žofka, see Ref. 13, p. 327.
- <sup>51</sup>V. N. Fetisov, see Ref. 13, p. 307.
- <sup>52</sup>T. Yamazaki, Enrico Fermi Summer School, Varenna, June 23–July 3 (1987), p. 78; INS-Rept.-658, Nov. (1987).
- <sup>53</sup>T. Motoba, H. Bandō, K. Ikeda, and T. Yamada, Prog. Theor. Phys. Suppl. No. 81, 42 (1985).
- <sup>54</sup>H. Bandō, see Ref. 9, p. 271c.
- <sup>55</sup>H. Bandō, J. Phys. Soc. Jpn. Suppl. **58**, 379 (1989).
- <sup>56</sup>V. G. Neudachin and Yu. F. Smirnov, *Nucleon Associations in Light Nuclei* [in Russian] (Nauka, Moscow, 1969).
- <sup>57</sup>V. G. Neudachin, *Proc. of the Intern. Conf. on Clustering Phenomena in Nuclei, Bochum, 21–24 July, 1969* (Intern. Atomic Energy Agency, Vienna, 1969), p. 35; Yu. F. Smirnov, *ibid.*, p. 153.
- <sup>58</sup>V. N. Fetisov, L. Majling, J. Žofka, and R. A. Eramzhyan, Z. Phys. A **314**, 239 (1983).
- <sup>59</sup>R. Wünsch, L. Majling, and J. Žofka, Czech. J. Phys. **B36**, 441 (1986); see Ref. 10, p. 329c.
- <sup>60</sup>D. E. Danskoī, Yad. Fiz. **49**, 63 (1989) [Sov. J. Nucl. Phys. **49**, 41 (1989)].
- <sup>61</sup>W. Brückner, M. A. Faessler, T. Ketel *et al.*, *Proc. of the Kaon Factory Workshop*, edited by M. K. Craddock, TRI-79-1 (Vancouver, August 13–14, 1979), p. 124.
- <sup>62</sup>L. Majling, in *Proc. of the International Seminar on the Theory of Few-Particle and Quark-Hadron Systems, June 16–20, 1987, Dubna* [in Russian], p. 405.
- <sup>63</sup>R. H. Dalitz and A. Gal, Phys. Rev. Lett. **36**, 362 (1976); Ann. Phys. (N.Y.) **131**, 314 (1981).
- <sup>64</sup>A. Bouyssy, Nucl. Phys. A**290**, 324 (1977); see Ref. 8, p. 413.
- <sup>65</sup>M. Rayet, Ann. Phys. (N.Y.) **102**, 226 (1976).
- <sup>66</sup>R. A. Eramzhyan, B. S. Iskhanov, J. M. Kapitonov, and V. G. Neudachin, Phys. Rep. **136**, 229 (1986).
- <sup>67</sup>J. Hüfner, S. Y. Lee, and H. A. Weidenmüller, Nucl. Phys. A**234**, 429 (1974).
- <sup>68</sup>V. A. Knyr, A. I. Mazur, and Yu. F. Smirnov, Ukr. Fiz. Zh. **32**, 1129 (1987).
- <sup>69</sup>R. Bertini, O. Bing, P. Birien *et al.*, Nucl. Phys. A**368**, 365 (1981).
- <sup>70</sup>A. Gal, J. M. Soper, and R. H. Dalitz, Ann. Phys. (N.Y.) **63**, 53 (1971).
- <sup>71</sup>A. Gal, J. M. Soper, and R. H. Dalitz, Ann. Phys. (N.Y.) **72**, 445 (1972).
- <sup>72</sup>A. Gal, J. M. Soper, and R. H. Dalitz, Ann. Phys. (N.Y.) **113**, 79 (1978).
- <sup>73</sup>M. I. Kozlov and V. N. Fetisov, Kratk. Soobshch. Fiz. No. 3, 68 (1971); No. 7, 16 (1971).
- <sup>74</sup>R. H. Dalitz and A. Gal, Ann. Phys. (N.Y.) **116**, 167 (1978).
- <sup>75</sup>E. H. Auerbach, A. J. Baltz, C. B. Dover *et al.*, Ann. Phys. (N.Y.) **148**, 381 (1983).
- <sup>76</sup>I. Talmi, Helv. Phys. Acta **25**, 185 (1952); M. Moshinsky, Nucl. Phys. **13**, 104 (1959); Yu. F. Smirnov, Nucl. Phys. **27**, 177 (1961); **39**, 346 (1962).
- <sup>77</sup>G. Racah, Phys. Rev. **76**, 1352 (1949).
- <sup>78</sup>G. Alexander, U. Karshon, A. Shapira *et al.*, Phys. Rev. **173**, 1452 (1968); B. Sechi-Zorn, B. Kehoe, J. Twitty, and B. Burnstein, Phys. Rev. **175**, 1735 (1968).
- <sup>79</sup>M. M. Nagels, T. A. Rijken, and J. J. de Swart, Phys. Rev. D **12**, 744 (1975); **15**, 2547 (1977).
- <sup>80</sup>B. W. Downs and R. J. N. Phillips, Nuovo Cimento **41A**, 374 (1966); **43A**, 454 (1966); R. H. Dalitz and F. Von Hippel, Phys. Lett. **10**, 153 (1964).
- <sup>81</sup>Y. Yamamoto, H. Bandō, and J. Žofka, Prog. Theor. Phys. **80**, 757 (1988).
- <sup>82</sup>F. Ajzenberg-Selove, Nucl. Phys. A**433**, 1 (1985); A**449**, 1 (1986); A**490**, 1 (1988).
- <sup>83</sup>L. Majling, J. Žofka, V. N. Fetisov, and R. A. Eramzhyan, Phys. Lett. **193**, 263 (1987).
- <sup>84</sup>D. Halderson, Phys. Rev. C **30**, 941 (1984).
- <sup>85</sup>K. Wildermuth and Y. C. Tang, *A Unified Theory of the Nucleus* (Vieweg, Braunschweig, 1977).
- <sup>86</sup>J. A. Wheeler, Phys. Rev. **52**, 1107 (1937).
- <sup>87</sup>Wang Xi-cang, H. Bandō, and H. Takaki, Z. Phys. A **327**, 57 (1987).
- <sup>88</sup>T. Yamada, K. Ikeda, H. Bandō, and T. Motoba, Phys. Rev. C **38**, 854 (1988); H. Bandō, Nucl. Phys. A**478**, 697c (1988).
- <sup>89</sup>F. Ajzenberg-Selove, Nucl. Phys. A**392**, 1 (1983).
- <sup>90</sup>T. Sakuda and H. Bandō, Prog. Theor. Phys. **78**, 1317 (1987).
- <sup>91</sup>L. Majling, J. Žofka, T. Sakuda, and H. Bandō, Prog. Theor. Phys. **79**, 561 (1988).
- <sup>92</sup>Yu. A. Simonov, Yad. Fiz. **3**, 630 (1966) [Sov. J. Nucl. Phys. **3**, 461 (1966)]; A. M. Badalyan and Yu. A. Simonov, Yad. Fiz. **3**, 1032 (1966) [Sov. J. Nucl. Phys. **3**, 755 (1966)].
- <sup>93</sup>R. I. Dzhibuti and Sh. M. Tsiklauri, Yad. Fiz. **36**, 1387 (1982); **43**, 1169 (1986); **45**, 670 (1987) [Sov. J. Nucl. Phys. **36**, 805 (1982); **43**, 748 (1986); **45**, 419 (1987)].
- <sup>94</sup>A. M. Gorbato, Yad. Fiz. **29**, 270 (1979); **36**, 602 (1982) [Sov. J. Nucl. Phys. **29**, 135 (1979); **36**, 350 (1982)].
- <sup>95</sup>B. F. Gibson, Nucl. Phys. A**489**, 115 (1988); B. F. Gibson and D. R. Lehman, Phys. Rev. C **37**, 679 (1988).
- <sup>96</sup>A. R. Bodmer, Q. N. Usmani, and J. Carlson, Phys. Rev. C **29**, 684 (1984); A. R. Bodmer and Q. N. Usmani, see Ref. 10, p. 257c.
- <sup>97</sup>N. N. Kolesnikov and V. I. Tarasov, Yad. Fiz. **36**, 815 (1982) [Sov. J. Nucl. Phys. **36**, 476 (1982)]; Izv. Vyssh. Uchebn. Zaved. Fiz. No. 5, 62 (1982); N. N. Kolesnikov and V. A. Kopylov, Izv. Vyssh. Uchebn. Zaved. Fiz. No. 5, 36 (1983).
- <sup>98</sup>Y. Tanaka, T. Motoba, and H. Bandō, see Ref. 12, p. 56.
- <sup>99</sup>W. H. Bassichis and A. Gal, Phys. Rev. C **1**, 28 (1970); J. Žofka, Czech. J. Phys. **B30**, 95 (1980); D. E. Lanskoī and T. Yu. Tret'yakova, Yad. Fiz. **49**, 401 (1989) [Sov. J. Nucl. Phys. **49**, 248 (1989)].
- <sup>100</sup>D. E. Lanskoī and T. Yu. Tret'yakova, Yad. Fiz. **49**, 1595 (1989) [Sov. J. Nucl. Phys. **49**, 987 (1989)].
- <sup>101</sup>Y. Yamamoto, Phys. Rev. C **36**, 2166 (1987).
- <sup>102</sup>J. Cohen and R. J. Furnstahl, Phys. Rev. C **35**, 2231 (1987).
- <sup>103</sup>C. Bennhold and L. E. Wright, Phys. Lett. **191B**, 11 (1987).
- <sup>104</sup>G. E. Walker, see Ref. 10, p. 287c.
- <sup>105</sup>C. G. Koutroulos and M. E. Grypeos, Phys. Rev. C **40**, 275 (1989).
- <sup>106</sup>J. D. Walecka, Ann. Phys. (N.Y.) **83**, 491 (1974); B. D. Serot and J. D. Walecka, Adv. Nucl. Phys. **16**, 1 (1986).
- <sup>107</sup>J. Cohen, Int. J. Mod. Phys. A**4**, 1 (1989).
- <sup>108</sup>C. B. Dover, Inst. Phys. Conf. Ser. No. 86, Paper presented at the Intern. Phys. Conf., Harrogate, UK (1986), p. 99.
- <sup>109</sup>V. A. Filimonov, see Ref. 7, p. 240.
- <sup>110</sup>J. C. Herrera, J. J. Kolata, H. W. Kraner *et al.*, Phys. Rev. Lett. **40**, 158 (1978).
- <sup>111</sup>R. E. Chrien, S. Bart, M. May *et al.*, Phys. Rev. C **41**, 1062 (1990).
- <sup>112</sup>L. Majling, J. Žofka, V. N. Fetisov, and R. A. Eramzhyan, Z. Phys. A **337**, 337 (1990).
- <sup>113</sup>M. Bedjidian *et al.*, Phys. Lett. **94B**, 480 (1980).
- <sup>114</sup>R. E. Chrien, *Proc. of the Intern. Symposium on Weak and Electromagnetic Interactions in Nuclei, Heidelberg, July 1–5, 1986*, edited by H. V. Klapdor (Springer Verlag, Berlin, 1986), p. 587.
- <sup>115</sup>R. E. Chrien, Concluding Talk, see Ref. 13, p. 727.

- <sup>116</sup>R. E. Chrien, Czech. J. Phys. B **39**, 914 (1989).
- <sup>117</sup>M. May, see Ref. 10, p. 179c.
- <sup>118</sup>Particle Data Group, Phys. Lett. **239B**, 1 (1990).
- <sup>119</sup>L. Pniewski and M. Danysz, Phys. Lett. **1**, 142 (1962).
- <sup>120</sup>N. N. Kolesnikov, G. A. Sokol, and D. Amarasingam, Preprint No. 61 [in Russian], P. N. Lebedev Physics Institute, Moscow (1981).
- <sup>121</sup>N. N. Kolesnikov, in *Abstracts of Papers at the International Symposium on the Theory of Few-Particle and Quark-Hadron Systems, June 16-20, 1987, Dubna* [in Russian], p. 109.
- <sup>122</sup>T. Y. Lee, S. T. Hsieh, and S. T. Chen-Tsai, Phys. Rev. C **2**, 366 (1970).
- <sup>123</sup>M. May, H. Piekarz, R. E. Chrien *et al.*, Phys. Rev. Lett. **47**, 1106 (1981).
- <sup>124</sup>D. Zieminska and R. H. Dalitz, Nucl. Phys. **B74**, 248 (1974).
- <sup>125</sup>S. Cohen and D. Kurath, Nucl. Phys. **73**, 1 (1965); **A101**, 1 (1967).
- <sup>126</sup>V. N. Fetisov, L. Majling, J. Žofka, and R. A. Eramzhyan, Preprint No. 112, FIAN, Moscow (1990).
- <sup>127</sup>F. C. Barker, Nucl. Phys. **83**, 418 (1966).
- <sup>128</sup>A. R. Bodmer and Q. N. Usmani, Nucl. Phys. **A450**, 257 (1986).
- <sup>129</sup>M. I. Kozlov and V. N. Fetisov, Preprint No. 25 [in Russian], P. N. Lebedev Physics Institute, Moscow (1974); V. N. Fetisov, M. I. Kozlov, and A. I. Lebedev, Phys. Lett. **38B**, 129 (1972); A. M. Bernstein, T. W. Donnelly, and G. N. Epstein, Nucl. Phys. **A358**, 195 (1981); S. S. Hsiao S. R. Cotanch, Phys. Rev. C **28**, 1668 (1983).
- <sup>130</sup>L. Majling, J. Žofka, V. N. Fetisov, and R. A. Eramzhyan, Physics with LAMPF II, Proposal, June 1983, LA-9798-P, Los Alamos Nat. Lab. (1983), p. 85; Phys. Lett. **130B**, 235 (1983); A. Gal, Phys. Rev. C **28**, 2186 (1983).
- <sup>131</sup>K. Itonaga, T. Motoba, and H. Bandō, Prog. Theor. Phys. **84**, 291 (1990).
- <sup>132</sup>V. V. Balashov, A. N. Boyarkina, and I. Rotter, Nucl. Phys. **59**, 417 (1964).
- <sup>133</sup>A. Bouyssy, Phys. Lett. **84B**, 41 (1979); Nukleonika **25**, 413 (1980).
- <sup>134</sup>M. Juric, G. Bohm, J. Klabuhn *et al.*, Nucl. Phys. **B52**, 1 (1973).
- <sup>135</sup>R. H. Dalitz and A. Gal, J. Phys. G **4**, 889 (1978).
- <sup>136</sup>V. N. Fetisov, L. Majling, J. Žofka, and R. A. Eramzhyan, Czech. J. Phys. **B36**, 451 (1986).

Translated by Julian B. Barbour